Front. Mech. Eng. 2022, 17(3): 37
https://doi.org/10.1007/s11465-022-0693-3

REVIEW ARTICLE

State-of-the-art on theories and applications of cable-driven parallel robots

Zhaokun ZHANG[a,b,c], Zhufeng SHAO (✉)[a,b], Zheng YOU[d], Xiaoqiang TANG[a,b], Bin ZI[e], Guilin YANG[f], Clément GOSSELIN[g], Stéphane CARO[h]

[a] *State Key Laboratory of Tribology, Department of Mechanical Engineering, Tsinghua University, Beijing 100084, China*
[b] *Beijing Key Laboratory of Precision/Ultra-Precision Manufacturing Equipment and Control, Tsinghua University, Beijing 100084, China*
[c] *Department of Mechanical Engineering, University of Michigan, Ann Arbor, MI 48109, USA*
[d] *Department of Precision Instrument, Tsinghua University, Beijing 100084, China*
[e] *School of Mechanical Engineering, Hefei University of Technology, Hefei 230009, China*
[f] *Ningbo Institute of Industrial Technology, Chinese Academy of Sciences (CAS), Ningbo 315201, China*
[g] *Department of Mechanical Engineering, Université Laval, Quebec QC G1V 0A6, Canada*
[h] *Laboratory of Digital Sciences of Nantes, National Centre for Scientific Research, Nantes 44321, France*

✉ *Corresponding author. E-mail: shaozf@mail.tsinghua.edu.cn (Zhufeng SHAO)*

© The Author(s) 2022. This article is published with open access at link.springer.com and journal.hep.com.cn

ABSTRACT Cable-driven parallel robot (CDPR) is a type of high-performance robot that integrates cable-driven kinematic chains and parallel mechanism theory. It inherits the high dynamics and heavy load capacities of the parallel mechanism and significantly improves the workspace, cost and energy efficiency simultaneously. As a result, CDPRs have had irreplaceable roles in industrial and technological fields, such as astronomy, aerospace, logistics, simulators, and rehabilitation. CDPRs follow the cutting-edge trend of rigid–flexible fusion, reflect advanced lightweight design concepts, and have become a frontier topic in robotics research. This paper summarizes the kernel theories and developments of CDPRs, covering configuration design, cable-force distribution, workspace and stiffness, performance evaluation, optimization, and motion control. Kinematic modeling, workspace analysis, and cable-force solution are illustrated. Stiffness and dynamic modeling methods are discussed. To further promote the development, researchers should strengthen the investigation in configuration innovation, rapid calculation of workspace, performance evaluation, stiffness control, and rigid–flexible coupling dynamics. In addition, engineering problems such as cable materials, reliability design, and a unified control framework require attention.

KEYWORDS cable-driven parallel robot, kinematics, optimization, dynamics, control

1 Introduction

Robots influence every aspect of our lives and have the potential to positively transform the world, improving efficiency, safety, and services. Considering the arrangement of joints and links, robots can be divided into two categories: serial and parallel robots. Most industrial robots are similar to the human arm, adopting a serial configuration (Fig. 1(a)). It is an open-loop structure with only one kinematic chain between the base and the end effector. Serial robots have the advantages of a large workspace and good flexibility, and the disadvantages of low load–weight ratio and low rigidity.

Received February 2, 2022; accepted April 10, 2022

In 1962, Gough and Whitehall [1] designed a six-degree-of-freedom (6-DOF) tire-testing machine with a parallel configuration. Later, Stewart [2] used a parallel mechanism for a flight simulator. This mechanism is called the Gough–Stewart platform [3] and is now widely used as a motion simulator. Parallel mechanisms have two or more kinematic chains connecting the base and end effector simultaneously. It is a closed-loop mechanism with passive joints (Fig. 1(b)). Parallel robots can be intuitively understood as multiple serial robots carrying the end effector together, exhibiting the potential for large rigidity, heavy loads, and high accuracy [4]. The actuation units of the parallel robot are frequently fixed to the static base, which results in low motion inertia and good dynamics [5]. These advantages of parallel mechanisms

triggered the machine tool revolution in the 1990s [6]. Parallel robots have also achieved commercial applications as motion simulators [7], pick-and-place robots [8], and spindle heads [9]. However, parallel robots are troubled with the small workspace, and complex singularities.

Cable-driven parallel robot (CDPR) is a special kind of parallel robot. CDPRs use several cables connect the base and end effector and drive the motion of the end effector by control the lengths of cables or the positions of the cable connection points [10]. The typical configuration of CDPR is shown in Fig. 1(c). Landsberger [11] first designed a 3-DOF CDPR for high-dynamic undersea operations in the 1980s and performed the mechanical analysis. CDPRs expand the workspace of parallel mechanisms greatly. In 1988, SkyCam developed a camera system driven by four cables that could travel at 13 m/s in a hundred-meter-scale workspace [12]. Based on the low cost, the outstanding advantages of CDPR lie in two aspects: large workspace with a high load capacity and high dynamics with a light weight.

CDPRs have an important role in various fields. One of the earliest and famous CDPRs is the RoboCrane robot developed by Albus et al. [13] at the National Institute of Standards and Technology (NIST) (Fig. 2 [14–17]). RoboCrane was extended to the fields of tensile truss robotic system [14], gantry and dual manipulator [15], aircraft maintenance [16], material handling [17], and underwater applications [18]. With excellent performance, RoboCrane was awarded the "Best of What's New" award as one of the 100 top products, technologies, and scientific achievements in 1992 [19].

The largest CDPR now is the Five-hundred-meter Aperture Spherical radio Telescope (FAST) [20], the world's largest telescope built in China (Fig. 3(a)). The FAST feed support system is a six-cable CDPR with a span of 600 m [21]. CDPRs are also a good option for warehousing and logistics. El-Ghazaly et al. [22] designed and developed the CoGiRo robot to implement auxiliary automation, such as palletizing, handling, auxiliary assembly, and spraying. The JASO Industrial Cranes developed the CraneBot that sums the advantages of smart cranes and parallel cable robotics to respond to the automation of industrial processes (Fig. 3(b)) [23]. In addition, due to its advantages of large workspace, good reconfigurable and rapid construction, CDPR has been applied in the construction field [24,25], such as bricklaying, exterior wall maintenance and painting. The Hephaestus project (Fig. 3(c)) is a good example [26,27]. Large space CDPRs are also used in the field of logistics and warehousing [28].

CDPRs have been successfully applied as high-load motion simulators, and they can be used to simulate acceleration in a large workspace. The CableRobot simulator developed by Miermeister et al. [29], combined with virtual reality technology, can be used for flight training and entertainment (Fig. 4(a)). CDPRs have also been adopted in wind tunnel simulations owing to their

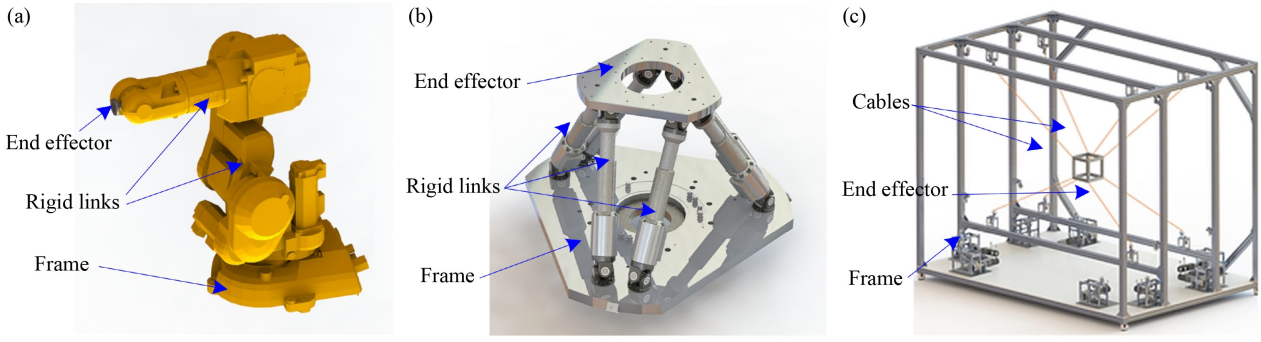

Fig. 1 Typical configurations of (a) serial robot, (b) parallel robot, and (c) cable-driven parallel robot.

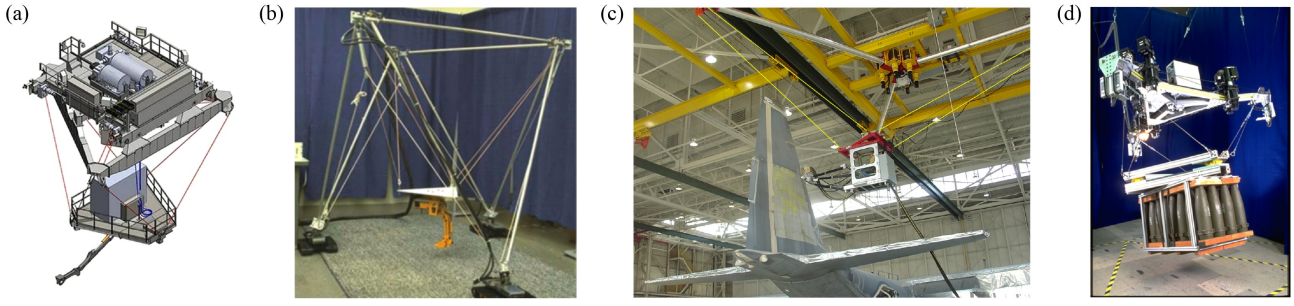

Fig. 2 RoboCrane technology used for (a) tensile truss robotic system [14], (b) gantry and dual manipulator [15], (c) aircraft maintenance [16], and (d) material handling [17]. Reprinted with permission from Refs. [14–17] from NIST.

advantages of low wind and water resistance. Bruckmann et al. [30] developed a cable-driven simulator for hydrodynamic experiments of hulls and submarines (Fig. 4(b)). ONERA in France designed the SACSO, a CDPR for wind tunnel tests of flight mechanics (Fig. 4(c)) [31].

The low cost and large workspace of CDPRs make them good options for large-space three-dimensional (3D) printing. Barnett and Gosselin [32] designed a suspended cable-driven 3D printer and constructed a 2.16-m-high statue of Sir Wilfrid Laurier (Fig. 5(a)). Zi et al. [33] and Qian et al. [34] designed a desktop 3D printer with parallel cable chains and achieved a 3-DOF translational motion (Fig. 5(b)). Pott et al. [35] designed the CaRo printer using four pairs of cables that formed parallelograms (Fig. 5(c)).

A cable is an excellent transmission and traction medium, and cable kinematic chains are similar to biological muscles. CDPRs have been applied in bionics and medical rehabilitation. Masiero et al. [36] designed the 3-DOF rehabilitation device in rehabilitation of post-stroke hemiplegic upper limbs (Fig. 6(a)). Surdilovic et al. [37,38] at the Fraunhofer Institute developed the String-Man for gait rehabilitation (Fig. 6(b)). Researchers at Columbia University developed a cable-driven exoskeleton system called CAREX [39,40] for upper limb rehabilitation (Fig. 6(c)).

Each coin has two sides. The flexibility, unidirectional force, and continuum characteristics of the cable pose challenges to the research and application of CDPRs and facilitate new theories and methods. Considering the weight and elasticity of the cables, statics and kinematics analysis of CDPR couple with each other and vibrations are important challenges for dynamics and control. Theories on configuration design, kinematics and dynamics modeling, performance evaluation and optimization, and motion control of CDPRs have been established.

This paper reviews and analyzes theoretical research on CDPRs. Challenges and future research prospects for

(a) (b) (c)

Fig. 3 CDPRs for lifting and handling: (a) FAST, reprinted with permission from Ref. [21] from Elsevier; (b) JASO CableCrane [23], © JASO Industrial Cranes; and (c) Hephaestus façade system, reprinted with permission from Ref. [27] from MDPI.

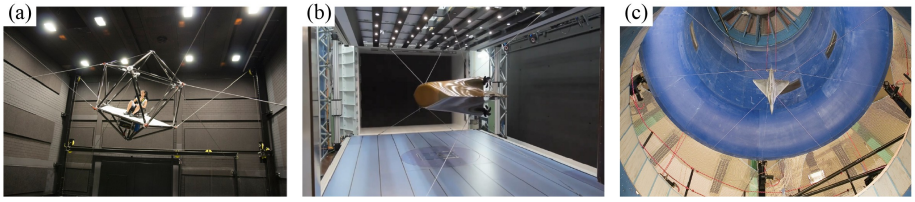

(a) (b) (c)

Fig. 4 CDPRs used for motion simulation and wind tunnel tests: (a) CableRobot simulator [29], © Max Planck Institute for Biological Cybernetics/Photographer: Miermeister P; (b) large low-speed wind tunnel for simulation of maneuvers [30], © Institute for Fluid Dynamics and Ship Theory at the Hamburg University of Technology; (c) SACSO wind tunnel for flight mechanics [31], provided and permitted by ONERA, French.

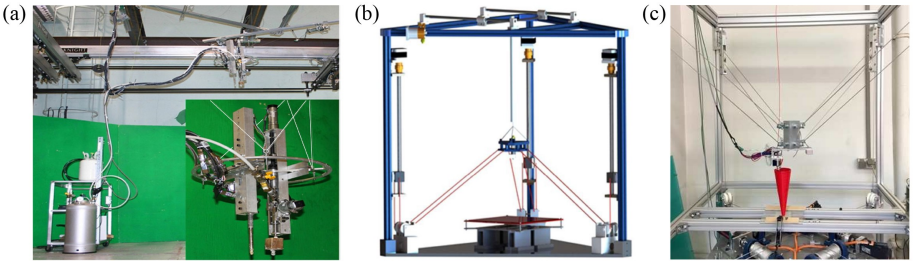

(a) (b) (c)

Fig. 5 CDPRs for 3D printing: (a) foam printer, reprinted with permission from Ref. [32] from Elsevier; (b) 3D printer with parallel-cable structure, reprinted with permission from Ref. [34] from MDPI; (c) CaRo printer, reprinted with permission from Ref. [35] from Springer Nature.

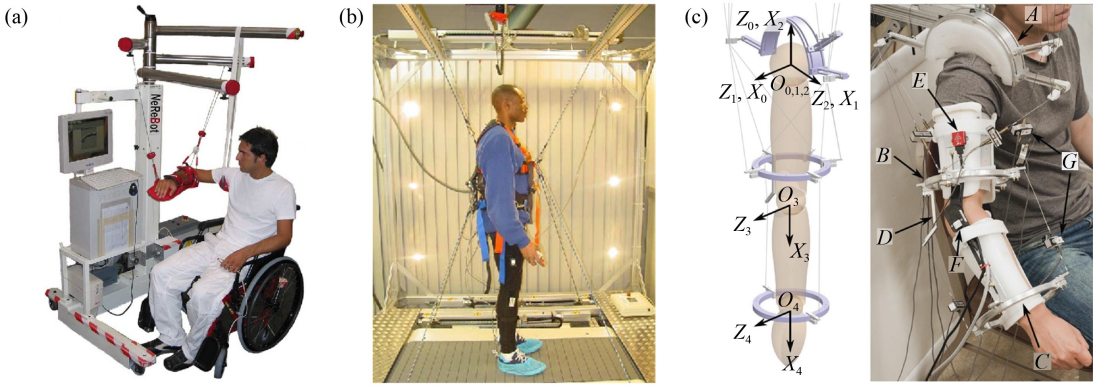

Fig. 6 CDPRs for rehabilitation: (a) the NeReBot used for upper limbs rehabilitation, reprinted with permission from Ref. [36] from Springer Nature; (b) String-Man for gait rehabilitation, reprinted with permission from Ref. [38] from Springer Nature; (c) CAREX for neural rehabilitation, © ROAR Lab at Columbia University, provided and permitted by Agrawal S K.

CDPRs are discussed. The remainder of this article is arranged as follows: Section 2 discusses the configuration design of CDPRs. Section 3 analyzes the kinematics and statics of CDPRs. Section 4 presents the performance evaluation and optimization methods for CDPRs. Section 5 reviews the dynamics of CDPRs. Section 6 discusses the control challenges. Finally, an outlook is provided in Section 7.

2 Configuration design

The CDPR is composed of a frame (base), cable chains, and an end effector (Fig. 7). Cable chains consist of actuators, guide pulleys, and cables. Cables are frequently wound on the winches (actuators) of the frame, guided by pulleys, and then connected to the end effector. The cable length between the cable outlet points A_i and cable connection points B_i changes with the rotation of the winches, thereby driving the motion of the end effector.

The configuration of a rigid robot refers to the arrangement of joints and links, which is the skeleton of a robot, determining its core kinematic performance and potential. The configuration design of CDPRs primarily focuses on the number and layout of the cables, and the key issue is whether the CDPR forms a tensegrity structure. The requirements of DOF are frequently the starting point of the configuration design. Owing to the unidirectional force characteristics of cables, the DOF analysis of CDPRs differs from that of rigid robots.

Ming and Higuchi [41] and Nguyen [42] first studied the configuration of CDPRs using the vector closure principle. Subsequently, Verhoeven [43] proved that CDPRs could realize six types of DOFs: pure translational motion of 1, 2, and 3 DOFs (1T, 2T, and 3T) with the point end effector, and the 2T1R, 3T2R, and 3T3R (T denotes translation and R denotes rotation) DOFs based on the nonpoint end effector (Fig. 8). Verhoeven [43] and Riechel et al. [44] established a configuration classification method for CDPRs considering the constraint capacity of cables to the end effector and defined the relationship between the number of driving cables (m) and the number of terminal DOFs (n). CDPRs are divided into four categories: under-constrained mechanism ($m < n$), incompletely constrained mechanism ($m = n$), fully constrained mechanism ($m = n + 1$), and redundantly constrained mechanism ($m > n + 1$). The under-constrained mechanism is seldom used because it cannot achieve a stable tensegrity structure, and the end effector has uncontrollable DOFs. For the CDPR in a fully constrained state, m must be greater than or equal to ($n + 1$) [45,46]. If gravity is considered a virtual cable, the incompletely constrained CDPR ($m = n$) can be considered a fully constrained CDPR ($m = n + 1$) with limited acceleration.

Ensuring that the cables are in tension is a prerequisite for CDPRs, which must be considered during the configuration design. From this perspective, CDPRs can be intuitively divided into two categories [47]. One is the cable-suspended parallel robots (CSPRs) which utilizes the gravity of the end effector and the load to maintain cables in tension. The CSPRs are incompletely constrained and achieve a fully constrained state through the gravity "cable" [48]. CSPRs are easy to build and control with a large workspace and heavy load capacity, which are generally used in spatial positioning and handling conditions. However, the terminal acceleration of a CSPR is limited. For fully constrained and redundantly constrained CDPRs, cable tension is ensured by arranging the cables on both sides of the end effector and pulling them against each other. A high stiffness and high-speed motion with significant acceleration can be achieved. Because m is greater than n, this results in actuation redundancy and an infinite cable-force distribution.

Recently, new types of CDPRs have emerged, which provide new approaches for innovative design. Some examples are shown in Fig. 9 [49–51]. As shown in Fig. 9(a), multi-link cable-driven robot was proposed by

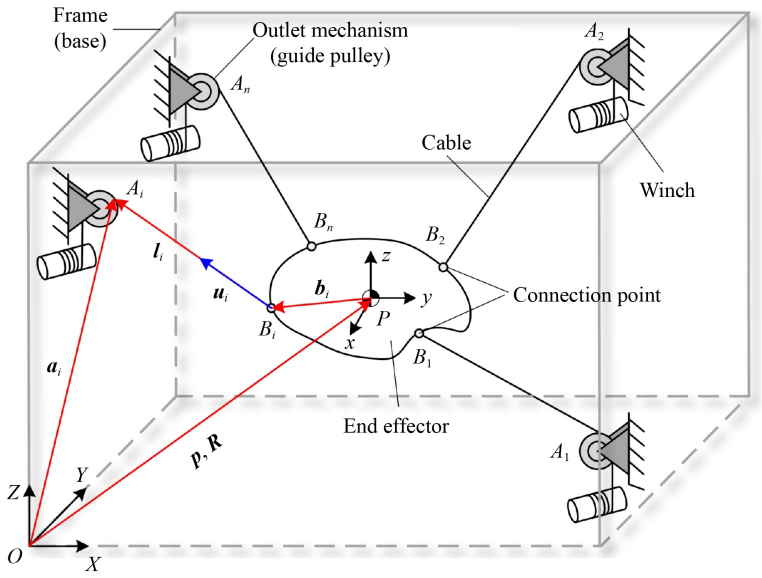

Fig. 7 Typical kinematic diagram of the CDPR.

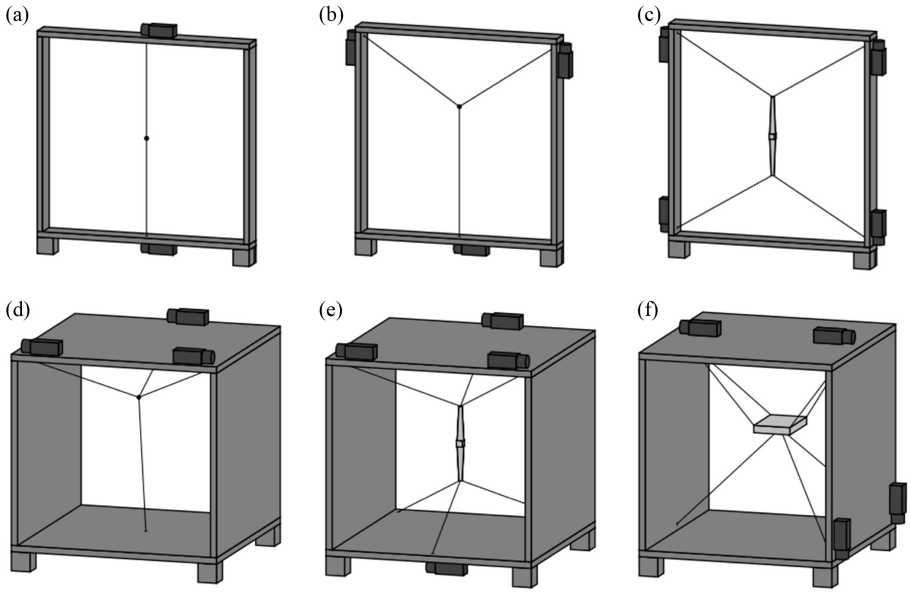

Fig. 8 Six types of DOFs for CDPRs [43]: (a) 1T, (b) 2T, (c) 2T1R, (d) 3T, (e) 3T2R, and (f) 3T3R.

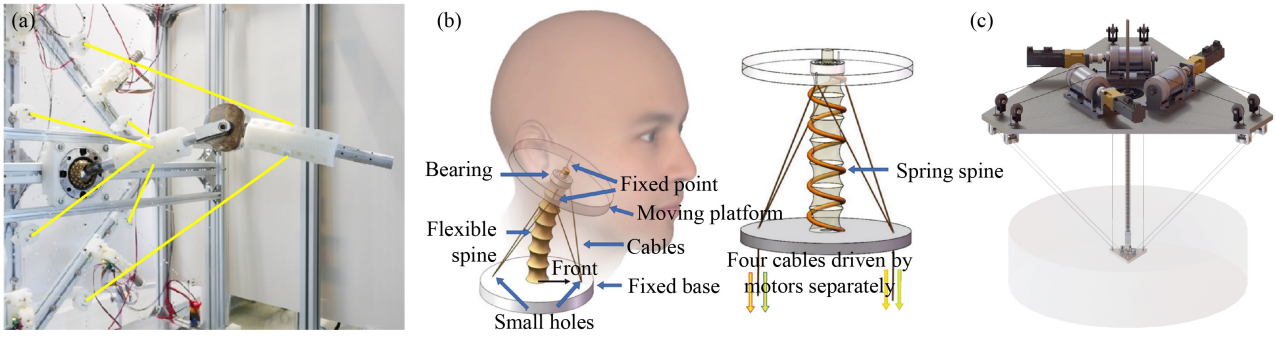

Fig. 9 CDPRs combined with multi-link, springs, and parallel-cable chains: (a) multi-link cable-driven robot, reprinted with permission from Ref. [49] from Springer Nature; (b) flexible parallel humanoid neck robot, reprinted with permission from Ref. [50] from Springer Nature; and (c) TBot robot.

combining the cable chain and serial rigid links [49,52], which are commonly used in bionic and rehabilitation [53,54]. Passive tensioning elements such as springs and cylinders were introduced into CDPRs to reduce the number of actuations and the control difficulty while ensuring complete constraints. The first CDPR with an auxiliary tensioning element was proposed by Landsberger and Sheridan [55], who used a central hydraulic cylinder in a 3-DOF CDPR to maintain cables in tension. Dekker et al. designed DeltaBot [56] and BetaBot [57] robots by adding passive air cylinders in the center. The cylinder is bulky and springs gradually become a preferred option in small-span CDPRs. The cable-driven humanoid neck robot (Fig. 9(b)) [50], and TBot high-speed pick-and-place robot (Fig. 9(c)) [51,58] have been proposed by adding springs in the central to keep cables in tension. In addition to tensioning cables, springs aid in expanding CDPR's workspaces [59,60] and optimizing the energy consumption during operation (springs can be used as energy storage elements) [61].

A drawback of cables is that it can only apply a unidirectional force to the end effector with little constraint. To improve the constraint ability of cables on the end effector, parallel-cable chains were proposed and translational CDPRs with nonpoint end effectors were established. The parallel-cable chain is a group of cables (frequently two cables) that are always parallel to each other during motion and form a parallelogram structure to constraint the rotations of the end effector [62]. Since parallel cables in the same group are wound and released simultaneously, they are generally driven by one actuator. Bosscher et al. [63] first used parallel cables in a rescue robot. Alikhani et al. [64] designed a large-space translational CDPR with parallel cables. Zi et al. [33] and Qian et al. [34] designed translational 3D CDPR printers (Fig. 5(b)). The parallel-cable chain effectively improved the constraint ability of the cables on the end effector and enriched the configuration and DOF form of the CDPRs.

In addition, utilizing cables as kinematic chains brings a strength to CDPRs, that is, the configuration can be easily reconstructed by rearrange the cables. Modular and reconfigurable characteristics of CDPRs provide significant flexibility to change their configuration and performance [65], which satisfies the requirements of high flexibility and efficient reengineering in modern manufacturing.

3 Kinematics and statics

3.1 Notations and kinematics

The kinematic model establishes the relationship between the cable length and pose of the end effector. Based on the massless and inelastic assumptions of the cable, the cable outlet and connection points on the base and end effector are considered fixed points. The point-to-point straight-line model is widely adopted in the kinematic modeling of CDPRs. As shown in Fig. 7, given the pose of the end effector, the length of each cable can be obtained as

$$l_i = \left\| \boldsymbol{a}_i - \boldsymbol{p} - {}^{O}\boldsymbol{R}_p \boldsymbol{b}_i \right\|, \; i = 1, 2, \ldots, m, \tag{1}$$

where l_i is the length of the ith cable, $\boldsymbol{a}_i$ is the position of cable outlet point A_i on the base, $\boldsymbol{p}$ is the position of the end effector, ${}^{O}\boldsymbol{R}_p$ is the rotation matrix of the end effector with respect to the base, and $\boldsymbol{b}_i$ is the position of the cable connection point B_i in the local coordinate system $\{P{-}xyz\}$.

The point-to-point straight-line model ignores two practical issues: the pulley in the cable chains and the shape of the cable. The cable outlet mechanism on the base of CDPRs has different structures and can be divided into four categories: the eyelet, single-pulley, double-pulley, and multi-pulley types [66] (Fig. 10). The eyelet type is an ideal scenario in which the cable outlet point is fixed. However, the relative motion between the cable and the eyelet produces severe friction and causes wear or breakage of the cable, resulting in low reliability and poor practicability.

Pulleys are frequently adopted in the outlet mechanism. The position of the cable outlet point at which the cable leaves the pulley changes with the pose of the end effector. The pulley can be equivalent to an RRP kinematic pair under the spatial conditions [67] or RP kinematic pair under planar conditions (P represents the prismatic joint). When the span of the CDPR is large and the pulley radius is small, the kinematic model based on the point-to-point assumption has acceptable accuracy. Otherwise, the point-to-point model results in apparent errors. Gonzalez-Rodriguez et al. [68] and Jin et al. [69] proposed a method of mounting compensation pulleys at the cable connection points of the end effector to counteract the errors; however, this method is primarily suitable for planar CDPRs in which the pulley does not swing or for low-speed spatial CDPRs.

A more general approach to improve the accuracy is to establish a complete kinematic model considering pulleys. A kinematic diagram of the CDPRs considering the pulley kinematics is shown in Fig. 11. When the pulleys are considered in the kinematic model, the tangent points and wrap angles of the cables on the pulleys should be calculated. Solutions for the kinematic modeling of the CDPR considering pulleys have been established [70]. The kinematic calibration method considering pulleys was also established [71], which thereby forms a complete solution for kinematics of CDPRs. The complete kinematics model with pulley kinematics significantly increases the positioning and trajectory accuracy of the CDPR. For example, the terminal accuracy of the IPAnema robot was increased by 21.6% [72,73].

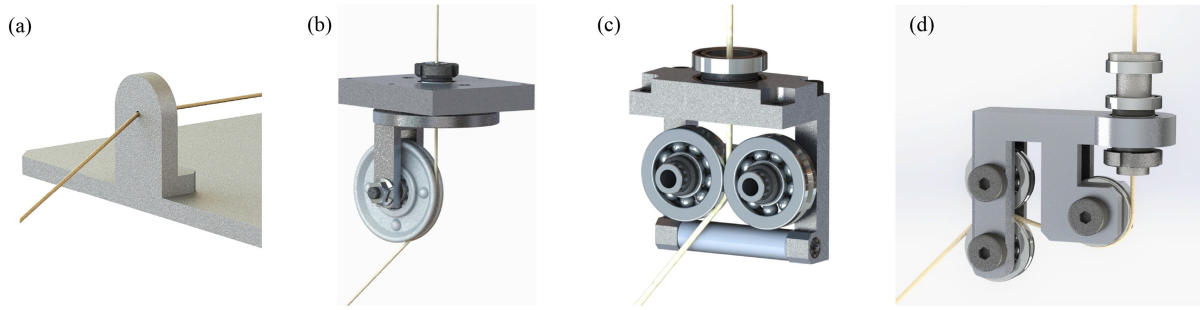

Fig. 10 Typical cable outlet mechanisms on the base: (a) eyelet type, (b) single-pulley type, (c) double-pulley type, and (d) multi-pulley type.

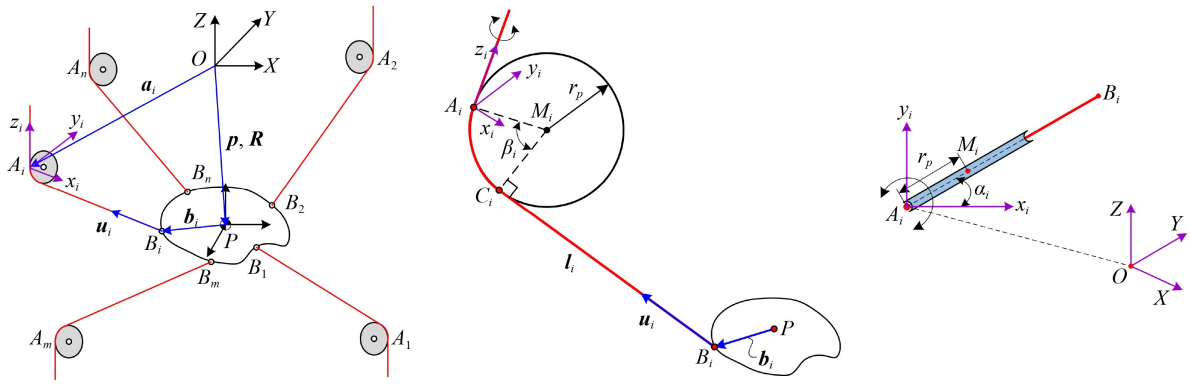

Fig. 11 Kinematic diagram of a CDPR considering the pulley kinematics.

In addition, the actual shape of cables needs to be considered in the CDPR kinematics. When the span of a CDPR is large and the weight of cables cannot be ignored, the cable's mass and elastic deformation will significantly decrease the accuracy of the point-to-point model. The kinematic modeling of a large-span CDPR requires consideration of the cable elasticity and mass. Based on the straight-line model, refined cable models such as the catenary and parabolic models have been proposed [74–76] (Fig. 12). The catenary model has a high accuracy, but the equation is nonlinear and requires iterative calculations. The complex calculation and time consumption make it difficult to use for real-time control. The parabolic model is an approximation of the catenary model and is significantly easier to solve with lower accuracy.

Compared with inverse kinematics, the forward kinematics of CDPRs are complicated without an explicit analytical solution. This is frequently solved by converting it into the optimization problem as

$$\boldsymbol{p} = \min(\boldsymbol{f}_{ik}(\boldsymbol{p},\boldsymbol{a}) - \boldsymbol{L}), \tag{2}$$

where $\boldsymbol{f}_{ik}(\boldsymbol{p},\boldsymbol{a})$ is the inverse kinematics of the CDPR, and $\boldsymbol{L}$ is the given vector of cable lengths. Numerical methods can be used to increase the calculation efficiency, such as the integral formula [77], interval analysis [78], and the Levenberg–Marquardt algorithm [79]. Pulley kinematics can also be considered in the forward kinematics of CDPRs [80,81].

Inverse kinematics are widely used because they are the basis of motion control and dimension design of CDPRs. Applications and research on forward kinematics that rely on numerical iteration are relatively few. The basic model of a cable is the point-to-point model. For refined kinematic modeling, it is necessary to consider the influence of cable sagging and the pulley mechanism.

3.2 Statics and cable force distribution

The basis of the CDPRs is the balance of the cable forces. When all the cables are tensioned, the force acting on the end effector by the ith cable is $t_i\boldsymbol{u}_i$, and the torque is $\boldsymbol{b}_i \times t_i\boldsymbol{u}_i$ (t_i represents the amplitude of the tension on the ith cable and $\boldsymbol{u}_i$ is the unit directional vector of the ith cable). The external force and torque acting on the end effector are denoted as $\boldsymbol{F}$ and $\boldsymbol{M}$, respectively, and the static equilibrium equation of the CDPR can be expressed as

$$\begin{bmatrix} \boldsymbol{u}_1 & \boldsymbol{u}_2 & \cdots & \boldsymbol{u}_m \\ \boldsymbol{b}_1 \times \boldsymbol{u}_1 & \boldsymbol{b}_2 \times \boldsymbol{u}_2 & \cdots & \boldsymbol{b}_m \times \boldsymbol{u}_m \end{bmatrix} \begin{bmatrix} t_1 \\ t_2 \\ \vdots \\ t_m \end{bmatrix} + \begin{bmatrix} \boldsymbol{F} \\ \boldsymbol{M} \end{bmatrix} = \boldsymbol{JT} + \boldsymbol{W} = 0, \tag{3}$$

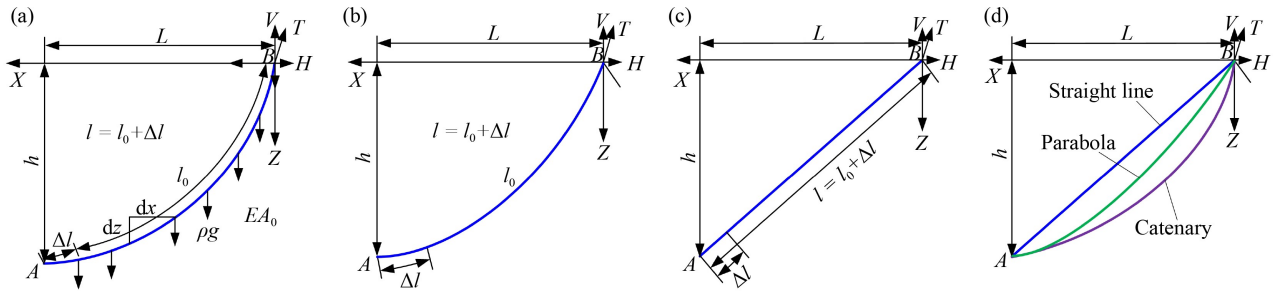

Fig. 12 Different cable models used in the kinematic modeling: (a) catenary model, (b) parabolic model, (c) straight-line model, and (d) comparison of different cable models.

where $\boldsymbol{J} = \begin{bmatrix} \boldsymbol{u}_1 & \boldsymbol{u}_2 & \cdots & \boldsymbol{u}_m \\ \boldsymbol{b}_1 \times \boldsymbol{u}_1 & \boldsymbol{b}_2 \times \boldsymbol{u}_2 & \cdots & \boldsymbol{b}_m \times \boldsymbol{u}_m \end{bmatrix}$ is the structure matrix of the CDPR, $\boldsymbol{W}$ is the external wrench acting on the end effector, and $\boldsymbol{T} = [\,t_1 \quad t_2 \quad \cdots \quad t_m\,]^{\mathrm{T}}$ is the cable-force vector of the CDPR.

The cable-force distribution of a CDPR is a matrix solution problem. The objective is to determine a positive force vector $\boldsymbol{T}$ that satisfies the equation of $\boldsymbol{JT} + \boldsymbol{W} = 0$ with the given pose of the end effector and the external wrench $\boldsymbol{W}$ applied to the end effector. This can be summarized as follows:

$$\begin{cases} \boldsymbol{JT} + \boldsymbol{W} = 0, \\ \text{s.t. } 0 < t_{\min} \leqslant t_i \leqslant t_{\max}, \end{cases} \tag{4}$$

where $t_{\min}$ and $t_{\max}$ are the minimum and maximum limits of the cable-force range, respectively. When the CDPR is nonredundant, a unique solution can be obtained by solving Eq. (4). For redundant CDPRs, because m is greater than n, the structure matrix $\boldsymbol{J} \in \boldsymbol{R}^{n\times m}$ is a nonsquare matrix, and there are infinite groups of solutions for the cable forces. The generic cable-force solution in Eq. (4) is

$$\boldsymbol{T} = \boldsymbol{J}^{+}\boldsymbol{W} + (\boldsymbol{I} - \boldsymbol{J}^{+}\boldsymbol{J})\lambda, \tag{5}$$

where $\boldsymbol{J}^{+} = \boldsymbol{J}^{\mathrm{T}}\left(\boldsymbol{J}\boldsymbol{J}^{\mathrm{T}}\right)^{-1}$ is the Moore–Penrose inverse of matrix $\boldsymbol{J}$, $\boldsymbol{I} \in \boldsymbol{R}^{m\times m}$ is the m-dimensional unit matrix, $(\boldsymbol{I} - \boldsymbol{J}^{+}\boldsymbol{J})\lambda$ is the homogeneous solution of the equation $\boldsymbol{JT} = \boldsymbol{W}$, $\lambda \in \boldsymbol{R}^{n}$ is an arbitrary vector, and $(\boldsymbol{I} - \boldsymbol{J}^{+}\boldsymbol{J})\lambda$ forms the zero-space vector of the structure matrix $\boldsymbol{J}$.

For redundant CDPRs, it is difficult to directly solve the cable force using the above equation. Therefore, the solution is converted into an optimization problem as follows:

$$\begin{aligned} &\text{objective function: optimize } \boldsymbol{G}(\boldsymbol{T}), \\ &\text{subjected to: } \begin{cases} \boldsymbol{JT} + \boldsymbol{W} = 0, \\ 0 < t_{\min} \leqslant t_i \leqslant t_{\max}, \end{cases} \end{aligned} \tag{6}$$

where $\boldsymbol{G}(\boldsymbol{T})$ is the target function. The optimization objective $\boldsymbol{G}(\boldsymbol{T})$ can be determined according to the requirements. The common optimization objectives are the minimum 1-norm or 2-norm of the cable-force vector $\boldsymbol{T}$. The minimum 1-norm optimization can be effectively solved using a linear programming method [82,83]. However, the obtained cable forces with the minimum 1-norm may have discontinuities when the end effector follows a continuous path. The minimum 2-norm optimization is frequently adopted with the bounded quadratic programming method [84,85]. Gosselin and Grenier [86] discussed the p-norm optimization thoroughly and explained the differences. If the order of the norm p is large, it will cause a dramatic change in the cable forces under a continuous trajectory. The 2-norm and 4-norm optimizations are preferred.

The cable force value obtained via the minimum p-norm optimization tends to be the minimum limit of the available range. If the cable force is small, the cable is prone to sagging. Relative p-norm optimization [86] was proposed to avoid this scenario. The mathematical expression of the relative p-norm optimization can be expressed as

$$\begin{aligned} &\text{objective function :} \\ &\text{optimize } \eta(\boldsymbol{t}) = \|\boldsymbol{t} - \boldsymbol{t}_{\mathrm{ref}}\|_p = \sqrt[p]{\sum_{i=1}^{m} \left|t_i - t_{\mathrm{ref},i}\right|^p}, \\ &\text{subjected to } \begin{cases} \boldsymbol{JT} + \boldsymbol{W} = 0, \\ 0 < t_{\min} \leqslant t_i \leqslant t_{\max}, \end{cases} \end{aligned} \tag{7}$$

where $t_{\mathrm{ref},i}$ is the target cable force of the ith cable. $t_{\mathrm{ref},i} = (t_{\min} + t_{\max})/2$ is often adopted [87]. In addition to the relative p-norm optimization, Lim et al. [88] used a tension index to adjust the cable forces to keep them away from the limits. Mikelsons et al. [89] proposed the gravity center of the plane of effective cable forces as the optimal solution.

When calculating the cable forces numerically, an important problem is time consumption considering the real-time control of the CDPR. Numerical iterative search methods based on the Karush–Kuhn–Tucker theory [90,91], improved gradient projection method [92], and interval analysis [93] have been proposed to increase the computational efficiency. Gradient-based optimization methods can frequently guarantee results within a particular period, but unpredictable nonconvergence may occur [93].

In addition to numerical calculation methods, geometric methods have been proposed for the cable-force

distribution problems of redundant CDPRs. Geometric methods primarily include the cable-force polygon method [94,95] and the gravity center method [89]. Combined with the gravity center method, several geometric cable-force optimization methods have been proposed based on the feasible region of the cable force. The feasible region of cable forces (which is frequently a cable-force polygon) should first be determined using the polygon method. Cui et al. [96] proposed a polygonal calculation algorithm that can effectively obtain the feasible region of cable forces based on the Graham scanning method.

In summary, the methods of solving cable forces for redundant CDPRs are divided into geometric and numerical methods. The p-norm numerical optimization method is the most commonly used. The relative p-norm optimization can adjust the target value of the cable forces to keep them far away from the force limits. The geometric method has some advantages such as simple calculation and avoiding iterations; however, it is currently only used for CDPRs with specific configurations and simple optimization objectives.

3.3 Workspace

The workspace is an important challenge in robot kinematics and applications. The workspace of a rigid robot is determined by the joints' motion range and chain size. Its workspace boundary is clear and can be usually expressed algebraically. The workspace of CDPRs is highly coupled with the cable forces. Various workspaces have been presented for CDPRs considering the constraints on the cable tension and external forces.

The static workspace is the most basic one, and it is defined as the set of poses that the end effector can attain and remain still with positive cable forces, with gravity as the only external force [97]. Subsequently, the wrench closure workspace (WCW) [98] and the force closure workspace (FCW) for the CDPRs with the point end effector [99] were proposed. The WCW is the pose set in which the CDPR can be balanced by a set of positive cable forces under an external wrench of any amplitude and direction. In the definition of the WCW or FCW, the external wrench and cable forces are not bounded. Considering the boundaries of cable forces and external wrench, Ebert-Uphoff proposed the concept of the wrench feasible workspace (WFW) [100,101], which is defined as the set of poses in which the end effector can generate or resist a particular range of wrenches with limited cable forces. For the CDPR with the point end effector, the WFW degenerates to the force feasible workspace (FFW) [102]. In addition, Verhoeven and Hiller [103] proposed a controllable workspace, and the physical meaning was equivalent to the WFW. Alikhani et al. [104] defined the tensionable workspace of CDPRs that is equivalent to the FCW. Barrette and Gosselin [105] proposed the concept of a dynamic workspace. The set of poses in which the end effector achieves dynamic balance under bounded acceleration and cable forces without external force is called the dynamic feasible workspace (DFW). Gagliardini et al. [106] further proposed an extended version of the DFW by considering the external wrench, centrifugal force, and Coriolis force. Shao et al. [107] realized the unification of dynamic and static workspaces based on the weak equivalence principle by combining the gravity and inertial force into an equivalent gravity.

Based on these definitions, the calculation methods for workspaces were established. Because the static workspace is simple, WCW and WFW are the primary focus. The null space method by solving the pseudo-inverse matrix [108] and the recursive method of matrix dimensionality reduction [99] have been proposed from an algebraic perspective. Zlatanov et al. [109] and Dong et al. [110] established a feasible solution method for WCW and WFW based on the convex set theory. Gouttefarde et al. [111] established a solution method for WFW based on interval analysis. Abbasnejad et al. [112] proposed a ray-based method for solving the WCW. The interval analysis and ray-based methods are essentially global search methods, which define the boundary of the workspace through interval dichotomy or rays. For CDPRs with a simple structure, the geometric and force vector closure methods are feasible and intuitive.

The analysis and solution of the dynamic workspace are coupled with the terminal acceleration of the CDPR, which converts the analysis and solution of the dynamic workspace into a trajectory-planning problem, and the research on dynamic workspace primarily focuses on CSPRs. Research on dynamic trajectory planning of CDPRs can be divided into three types: periodic, point-to-point motion, and transition trajectory planning [113–115]. The planning of the dynamic trajectory primarily focuses on the feasibility of the trajectory. The commonly used trajectory forms are the polynomial and trigonometric function approximations of the pendulum trajectory [116,117]. The performance of the dynamic trajectory can be gradually considered [107], such as the stability of the trajectory and the time–energy optimal principle.

Generally, the workspace of CDPRs is more challenging than that of rigid mechanisms, which are highly coupled with the cable forces and fundamentally determined by the configuration. The WCW is an ideal workspace that does not consider the boundary constraints of cable and external forces. The WFW is more practical, and its calculation methods are the primary focus. The cable-force distribution is dependent on the selection of the solution method, and the workspaces obtained with different cable-force solution methods could be variant. The establishment of the dynamic workspace further expands the motion range of the end effector and transforms the analysis of the workspace into the solution of the trajectory.

3.4 Stiffness

The stiffness of the CDPRs is also associated with the cable forces. The cable-force distribution affects the stiffness matrix [118]. In early research, the spring model of the cable was used to establish the stiffness model of the CDPRs [119]. More accurately, the stiffness of a CDPR should be defined by the motion vector of the end effector caused by the wrench acting on it. When there is a slight change on the wrench ($\mathrm{d}\boldsymbol{W}$), it will inevitably cause a corresponding small motion of the end effector ($\mathrm{d}\boldsymbol{X}$), and the stiffness matrix of the CDPR ($\boldsymbol{K}$) is defined as

$$\boldsymbol{K} = \frac{\mathrm{d}\boldsymbol{W}}{\mathrm{d}\boldsymbol{X}} = -\frac{\mathrm{d}\boldsymbol{J}}{\mathrm{d}\boldsymbol{X}}\boldsymbol{T} - \boldsymbol{J}\frac{\mathrm{d}\boldsymbol{T}}{\mathrm{d}\boldsymbol{X}} = \boldsymbol{K}_1 + \boldsymbol{K}_2. \tag{8}$$

The stiffness of the CDPR consists of two parts. $\boldsymbol{K}_1 = -\frac{\mathrm{d}\boldsymbol{J}}{\mathrm{d}\boldsymbol{X}}\boldsymbol{T} = \boldsymbol{H}\boldsymbol{T}$ is the static stiffness determined by the configuration, pose of the end effector, and cable forces, $\boldsymbol{H} = -\frac{\mathrm{d}\boldsymbol{J}}{\mathrm{d}\boldsymbol{X}}$ is the Hessian matrix. $\boldsymbol{K}_1$ is called the geometric stiffness matrix [120] or the active stiffness [121], which is related to the cable forces. The key to obtaining $\boldsymbol{K}_1$ is to calculate the Hessian matrix $\boldsymbol{H}$. Cui et al. [122] introduced an analytical method of deducing the Hessian matrix based on line geometry and directional cosines. Surdilovic et al. [120] and Yeo et al. [123] proposed the calculation results of $\boldsymbol{H}$ based on Kronecker's product or tensor product.

$\boldsymbol{K}_2 = -\boldsymbol{J}\frac{\mathrm{d}\boldsymbol{T}}{\mathrm{d}\boldsymbol{X}}$ represents the stiffness generated by the change in the pose of the cables, which is called the cable stiffness matrix, also known as the passive stiffness. $\boldsymbol{K}_2$ depends on the configuration, pose of the end effector, and material properties of the cable. Compared with $\boldsymbol{K}_1$, the solution of $\boldsymbol{K}_2$ is much simpler, and is expressed as follows:

$$\begin{aligned}\boldsymbol{K}_2 &= -\boldsymbol{J}\frac{\mathrm{d}\boldsymbol{T}}{\mathrm{d}\boldsymbol{X}} = -\boldsymbol{J}\frac{\mathrm{d}\boldsymbol{T}}{\mathrm{d}\boldsymbol{L}}\frac{\mathrm{d}\boldsymbol{L}}{\mathrm{d}\boldsymbol{X}} \\ &= \boldsymbol{J}\,diag\begin{pmatrix} \frac{E_1A_1}{l_1} & \frac{E_2A_2}{l_2} & \cdots & \frac{E_mA_m}{l_m} \end{pmatrix}\boldsymbol{J}^{\mathrm{T}},\end{aligned} \tag{9}$$

where E_i and A_i are the elastic modulus and cross-sectional area of the ith cable, respectively.

In redundant CDPRs, there are infinite solutions for the cable forces, which enables the adjustment of the stiffness of the CDPR through the cable-force distribution [124,125]. Cui et al. [122,126] studied the controllable stiffness of a CDPR based on static stiffness analysis and cable tension distribution to increase the stiffness consistency in the workspace. The variable stiffness device (VSD) has been designed to fine-tune and reduce the stiffness of the CDPR [123,127,128]. The VSD is generally composed of spring and rigid components embedded in the cable chain. In large-span CDPRs, the cable kinematics and force differ from those of small-span CDPRs because of the influence of the weight and flexibility of cables, and the stiffness changes. Du et al. [129], Yuan et al. [130], and Arsenault [131] explored the significant influence of cable mass and deformation on the stiffness of large-span CDPRs.

In summary, the basis of the design and analysis of CDPRs is the balance of the cable-force system, which is completely different from the kinematic analysis of rigid robots. The workspace, kinematics, and stiffness of the CDPRs are all related to the distribution of the cable forces. Currently, the cable-force distribution methods primarily solve the problems of feasibility and continuity of cable forces; however, research on the impact of the cable-force distribution on the performance (such as the ability to resist external forces, cable deformation, and terminal errors) is imperfect.

4 Performance evaluation and optimization

Dimensional optimization is an important method for a robot to obtain a good kinematic performance. The performance evaluation index is the standard for optimization, which makes the designs quantitatively comparable. Based on this, an optimization design method can be established using suitable mathematical tools, and the objective function is constructed with different performance indices.

The volume or area of the workspace is the most basic and commonly used performance index for the optimization of CDPRs [132–134]. However, it is often insufficient if only the size of the workspace is measured because there could be locus with poor performance inside the workspace. Indices used to measure the quality of the workspace have been proposed. The most common method is to adopt the conditioning number and dexterity indices of the parallel robots [135–137] to determine the global conditioning number and dexterity in the workspace based on the workspace size.

Cable-force distribution and stiffness indices have also been proposed for CDPR optimization. Yang et al. [138] defined the index of the tension factor, which equals the ratio of the minimum cable force to the maximum cable force in the workspace. The tension factor was used to evaluate the quality of the FCW of a fully constrained CDPR. Duan et al. [139] proposed a standard deviation of cable forces in the workspace. Tang et al. [140] proposed an index as the variance of the cable forces over the minimum tension. The uniformity of the cable forces [141,142] is often adopted as an optimization objective. In cable-driven rehabilitation robots, minimizing the maximum cable force is important because cable forces that act on the human body affect comfort and safety [143–145]. Shao et al. [146] evaluated the force exerted

by a cable-driven exoskeleton on an arm by defining the maximum force index (MFI) and average force index (AFI). The dimensional parameters of the cable-driven exoskeleton were optimized using the MFI and AFI indices with the atlas method.

The stiffness of CDPRs is relatively low, and optimization is often performed to increase the stiffness [147–149]. To evaluate the stiffness performance, Li and Xu [150] proposed an overall stiffness index. Cui et al. [151] proposed the concept of constant stiffness space (CSS) and used the maximum CSS as a performance index to optimize the parameters of the CDPR through the response surface model.

Specific and effective indices have been proposed for special types of CDPRs. Gouttefarde et al. [152] defined an index for heavy-duty CSPRs considering the maximum acceptable distance between the mobile platform geometric center and the payload mass center. Zhang et al. [51] defined the orthogonality-based local actuation index and the orthogonality-based local constraint index based on the orthogonality of the terminal actuation and constraint forces. The kinematic parameters of the high-speed TBot robot were optimized using the atlas method. Currently, orthogonality-based indices are only applicable to nonredundant CDPRs.

The optimal design of a CDPR is often a multi-objective optimization problem. Genetic and particle swarm algorithms have been widely adopted [143–145]. Jamwal et al. [153] proposed an evolutionary algorithm-based nondominated sorting algorithm for multi-objective optimization problems. Scholars from Tsinghua University often use the atlas method to optimize designs [51,154]. The atlas method visually displays the value variations of indices with the design variables to superimpose and select the optimal design parameters. However, the atlas method is only applicable when the number of parameters does not exceed three.

In summary, the existing performance evaluation indices for CDPRs primarily involve the workspace, dexterity, cable-force distribution, and stiffness. In fully and redundantly constrained CDPRs, the indices of stiffness and workspace are determined based on cable forces. It is necessary to determine the cable-force distribution method before performing the analysis and optimization, and the workspace and stiffness indices cannot be decoupled from the cable force. The aim of the performance evaluation is to rapidly determine the advantages and disadvantages of the configuration. The performance index should have a clear and unique value for a certain configuration. The Jacobian matrix and orthogonality-based indices can achieve this objective, but they are primarily used for nonredundant CDPRs. Performance indices and optimization design methods that are decoupled from cable forces should be studied in the future.

5 Dynamics

The key to CDPR dynamics is the modeling of cables. Considering the span and mass of cables as well as CDPR configurations, there are mainly four types of cable dynamic models: the massless inelastic, massless elastic, continuous mass elastic, and distributed mass (or concentrated mass) elastic cable models.

In early research on the dynamic modeling of CDPRs, the massless inelastic cable model was used, and the cable mass and elasticity were ignored. The dynamic model of the CDPR is simplified to the dynamics of the end effector under cable and external forces. The Newton–Euler method [155], virtual work principle [156], Lagrangian method [157], and Kane's method [158] are used to build the dynamic model.

Furthermore, axial linear or nonlinear springs have been used for the elastic deformation modeling of cables under tension [159]. The massless elastic cable model is often used to model fully or redundantly constrained CDPRs with small spans [160], such as the BetaBot [118] and IPAnema [161]. Damping can be included, and the spring–damping model has been widely used in CDPRs [162–164]. In addition, the hysteresis and creep behaviors [165] can also be included in the spring–damping model. Choi and Park [166] proposed an integrated nonlinear dynamic model of a polymer cable, and dynamic behaviors, such as the nonlinear elongation, hysteresis, creep, and short-term and long-term recovery, were described with the integrated nonlinear dynamic model based on the viscoelastic model.

For large-span CSPRs, the mass of the cable causes significant differences in the magnitude and direction of the cable force and results in significant modeling differences. A continuous-mass elastic cable model and a distributed mass (or concentrated mass) elastic cable model were proposed for large-span CSPRs to describe the dynamic characteristics caused by the self-weight and sagging effects of long cables [167] (Fig. 13).

The continuous-mass elastic cable model corresponds more with actual CSPRs. The catenary or parabola [75,168] is generally used to describe the shape of a cable. The finite element method (FEM) and the integral method are used for the dynamic modeling of continuous-mass or distributed-mass cables. The FEM is more popular because it is mature and intuitive [169–172]. Tempel et al. [173] proposed a modified rigid-body FEM based on a rigid body and spring–damping elements and established a multi-body dynamics model of a planar 3-DOF CDPR.

Ottaviano and Castelli [167] studied and compared four types of cable models and indicated that the key to selecting a suitable cable model is to solve the ratio of the end-effector mass to the cable mass or the ratio of the wrench on the end effector to the cable forces. The core is

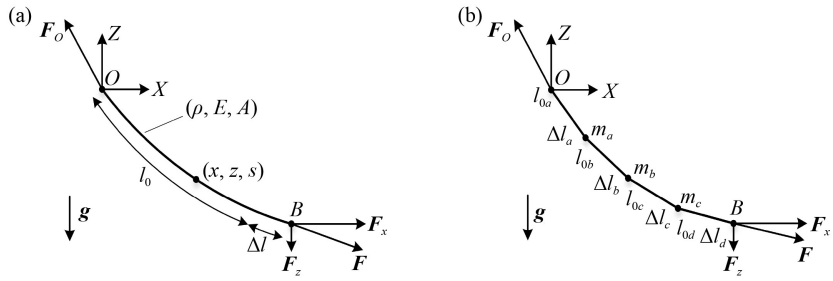

Fig. 13 (a) Continuous-mass elastic cable model and (b) distributed-mass elastic cable model.

the balance between accuracy and model complexity. In addition, as mentioned in Section 2, rigid–flexible coupling or hybrid CDPRs were gradually designed and used. In the modeling of these new types of CDPRs, rigid–flexible coupling problems are encountered. The efficient modeling method of the rigid–flexible coupling model will be an important research direction in the future.

The vibration of the CDPR occurs owing to the elasticity of cables. Based on the elastic dynamic model, time-domain and frequency-domain vibration analyses can be performed. Three methods are commonly used in the vibration or stiffness analysis of CDPRs: (1) analytical analysis based on the simplified elastic model of CDPRs, (2) FEM, and (3) dynamic stiffness method. Diao and Ma [159] analyzed the vibration of a fully constrained CDPR based on the spring string vibration model and indicated that the transverse vibration of cables can be ignored compared with the axial flexibility of cables for CDPRs. This conclusion confirms the reliability of the cable model as a longitudinal spring. Shao et al. [164] and Liu et al. [174] analyzed the dynamic characteristics of the low-order natural frequency and mode shape of the feed support system of the FAST, based on the spring–damping concentrated mass model. The FEM is primarily used to analyze the vibration and mode of CDPRs under the conditions of distributed and continuous mass cable models [175,176]. The accuracy of FEM depends on the number of elements; therefore, a strong trade-off exists between accuracy and computational burden. Yuan et al. [177] proposed a vibration analysis method based on a dynamic stiffness matrix. The dynamic stiffness matrix method provides better accuracy than the FEM because it relies on frequency-dependent shape functions that are exact solutions of the governing differential equations.

For nonredundant CDPRs (primarily CSPRs), the FEM, continuous-mass-based catenary model, or parabolic model can solve the dynamics modeling problems well. However, for fully or redundantly constrained CDPRs, dynamic modeling and vibration analysis are more difficult because they involve cable-force distribution and deformation coordination conditions. In addition, there are also differences in the vibration characteristics of the two types of CDPRs. The vibration of the large-span CSPRs is primarily reflected in the low frequency and large amplitude, while the small-span redundant CDPRs are more manifested in the higher-frequency vibration. This results in differences in the vibration suppression control methods, which will be discussed in the following section.

6 Control

6.1 Motion control

Control is the guarantee that the robot can achieve the required function. The most common method is kinematics-based cable length control [178], such as proportional–integral–derivative (PID) control based on the feedback of the motor encoder. Ensuring sufficient positive cable forces and the effectiveness of the kinematics control model are the primary challenges in the control of CDPRs [179]. However, owing to the self-weight and flexibility of cables, nonlinear and time-varying characteristics exist in the mapping of the encoder feedback and cable length. Closed-loop position feedback has been used in large-span CDPRs to increase the accuracy of kinematic control [180,181]. In addition, Shang et al. [182] studied the synchronization error of CDPRs in the cable space and designed a synchronization controller to realize the coordinated movement between the cables and ultimately increase the tracking accuracy of the end effector.

The elasticity of the cable interconnects the length deformation and cable force, which means that the cable force can be adjusted through cable length control in kinematics. Based on kinematic control, a dynamic or an electrostatic model can be adopted to establish the feedforward controls (Fig. 14(a)). The dynamic model can be adopted to predict the cable force based on the motion status and adjust the cable length accordingly [183]. In addition, the cable force can be measured using sensors, and the cable lengths are adjusted according to the cable force deviation [175], avoiding cable sagging [184]. Baklouti et al. [185] studied a feedforward control scheme based on an elasto-dynamic model that could

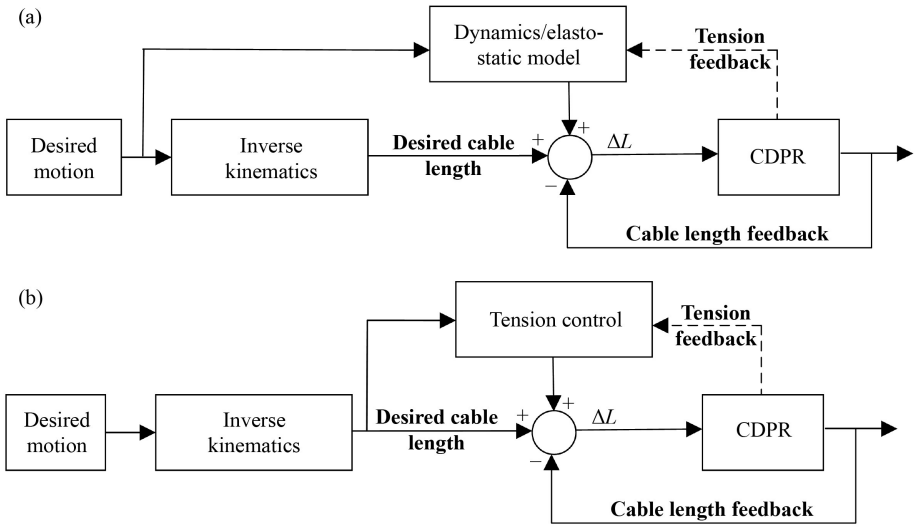

Fig. 14 Control block diagram of (a) feedforward control based on kinematics and (b) cascade control based on kinematics.

reduce the vibration caused by the elasticity of the cables. When the length and force of the cables are measured, cascade control can be established (Fig. 14(b)). The dynamic or cable-force control logic can be rearranged as a secondary controller to receive the output of the kinematic model and control the cable length. Abdelaziz et al. [186] discussed a cascade position control strategy for CDPRs with an internal cable-force control loop.

Model-based controls require accurate parameters. However, owing to the existence of uncertainty and error, some parameters in the models cannot be accurately determined or obtained. In such scenarios, nonlinear and intelligent control methods that do not rely on accurate models have been adopted, such as fuzzy and adaptive control. For an improvement in the traditional PID control, fuzzy PID controllers have been developed and used [187,188] to adjust the gain parameters more robustly when encountering disturbances and parameter uncertainties. Fuzzy sliding-mode controllers have also been used. For example, Zi et al. [189] established an adaptive fuzzy sliding mode controller for a hybrid CDPR. Babaghasabha et al. [190,191] designed an adaptive robust sliding mode controller based on the upper limit of uncertainty and a composite robust controller based on singular perturbation theory to counteract the unstructured and parameter uncertainties of CDPRs. Tajdari et al. [192] proposed the robust control of a 3-DOF CDPR with an adaptive neuro-fuzzy inference system. The developed PID controller was used to provide a learning dataset for training a neural network. The well-trained network was used to control the CDPR. Jabbari Asl and Janabi-Sharifi [193] developed a new nonlinear controller with a learning ability to compensate for modeling uncertainty that adopted an adaptive multi-layer neural network to solve time-varying external interference.

In addition to the above-mentioned controllers, performance-enhanced controllers based on specific CDPRs have also been developed. Yu et al. [194] studied an enhanced trajectory-tracking control with active stiffness control. The controller implements stiffness adjustment in the workspace by optimizing the cable-force distribution. Zarei et al. [195] proposed the concept of phase trajectory length and oscillation index and used new concepts to optimize the controller gain parameters to reduce the oscillation of a system. Jamshidifar et al. [196] studied the vibration decoupling modeling and robust control of redundant CDPRs and used linear parameter-varying (LPV)-H_∞ control to suppress the adverse effects of external interference on the trajectory tracking performance of the end effector.

6.2 Vibration suppression control

Vibration suppression is a key and challenging problem in both the theory and application of CDPRs. These methods can be divided into two categories: passive and active vibration suppression. Passive vibration suppression uses the damping and friction of the robot itself to dissipate the vibration energy. Because the efficiency is low, the robot usually pauses the motion and cannot guarantee a continuous movement of the end effector. Extra dampers can be added to accelerate the dissipation of vibration energy [197–199], but they are only efficient for the vibration of a pre-designed target frequency and are difficult to apply to CDPRs whose vibration characteristics vary with terminal poses.

Active vibration suppression restricts the vibration amplitude within a limited range by implementing active continuous control, which does not interrupt the movement of the CDPR and is the main method used. Active vibration suppression primarily uses three methods: pose compensation, internal force, and input filtering. Pose compensation is achieved by directly or

indirectly measuring the end-effector error in real time and transforming the error into the cable space of the robot to perform kinematic compensation [200,201] or adopting an additional small robot [202]. Internal force vibration suppression eliminates or reduces the vibration of the end effector by controlling the cable forces or the reaction force of an additional mechanism. Rushton and Khajepour [203] proposed a control strategy to eliminate out-of-plane vibrations in a planar CDPR by controlling the cable forces. de Rijk et al. [204] and Rushton et al. [205] proposed a vibration control method that adds a multi-axis response system to a planar CDPR. When the rigid pendulum swings, it generates a reaction force and torque on the end effector to achieve vibration suppression. Input filtering, also known as input shaping, is an open-loop control technique that eliminates self-excited vibrations at a certain frequency. Korayem et al. [206] used a robust input shaper to prevent the excitation of natural modes. Montgomery and Vaughan [207] used a dual-mode zero-vibration–extra-insensitive shaper to reduce the vibration of suspended SkyCam robots.

Large-span CDPRs usually have lower frequencies and narrower control bandwidths, which are more prone to low-frequency and large-amplitude vibrations. Therefore, an additional mechanism is frequently required to perform pose compensation or internal force vibration suppression. For small-span CDPRs, while most of them are redundant CDPRs, they have higher vibration frequencies and a wider control bandwidth. Vibration suppression methods that control cable lengths or forces are applicable.

Control is the main method used to determine the function and performance of CDPR and has become the focus of research in the field of CDPRs. Model-based feedforward control, feedback linearization, cascade control, and adaptive robust control appear one after another. It is foreseeable that fuzzy control, adaptive control, and even intelligent control will become the mainstream of future research with increased accuracy requirements and an in-depth analysis of the system uncertainty and nonlinear factors. Vibration is an eternal topic of CDPRs and is a main factor that limits the application of CDPRs. The efficient vibration control of CDPRs is an important breakthrough in its applications.

7 Outlook

As a novel type of parallel robot, CDPRs use cables instead of rigid chains to drive the end effector, which embodies the high-performance development trend of robots, reflects the advanced lightweight concept, and has inherent superiority in rigid–flexible fusion and serial–parallel hybrid configurations. CDPRs have significant advantages such as large workspace, low inertia, high dynamics, low cost, simple structure, and easy reconstruction, with successful applications in various fields. Additionally, the unidirectional force characteristics of the cable result in tension constraints and uniqueness in the configuration design, while cable flexibility challenges the modeling and control of CDPRs. The future research and application prospects of the CDPRs are shown in Fig. 15.

Generally, cables are good at transmission and weak at constraints. The configuration composed of only cable chains is limited. The configuration and DOFs are enriched by adopting new structures. The combination of rigid chains, parallel cables, and passive tensioning elements improves the performance and practicability of CDPRs and has become an emerging trend in configuration design. Parallel cables and rigid chains can improve the constraint capability, while passive tensioning elements can prevent actuation redundancy. In the future, hybrid CDPRs will become popular, and they can be closely integrated with bionics. Moreover, inspired by bionics, high-redundancy CDPRs can be a potential solution for more efficient and compact structures. Reconfigurable and modular CDPRs will also be a direction for future research and application of CDPRs.

Effective static analysis and cable-force distribution methods have been proposed to ensure positive and bounded cable forces. Because the cable forces directly affect the performance, vibration, and control of the CDPRs, more factors should be considered in the cable-force distribution based on real-time requirements. The solution of cable forces with more reasonable constraints should be explored, such as the energy efficiency, uniformity of cable forces, and stiffness. The polygon methods focus on a rapid determination of the vertices of the feasible region of the cable-force polygon according to the configuration of the CDPR. A method to perform multi-objective optimization would also be meaningful.

The workspace of CDPRs is more challenging than that of rigid mechanisms, which are highly coupled with cable forces. Performance indices that are decoupled from the cable force and directly based on configuration require further in-depth research, which will create the foundation for optimized designs. Coupling with the cable force provides an approach for the stiffness adjustment. The stiffness modeling of cable-driven multi-body robots and hybrid CDPRs requires further research. Stiffness adjustment based on the cable-force distribution still lacks precise quantitative research and is worth investigating in the future.

As the performance requirements of the robot increase, the accuracy of the kinematic and dynamic models of CDPRs continues to improve with the pulley kinematics and the continuous-mass elastic cable model. Considering the configuration innovation, the modeling of rigid–flexible coupling hybrid CDPRs will be an important research direction in the future. The balance of accuracy and model complexity should be considered

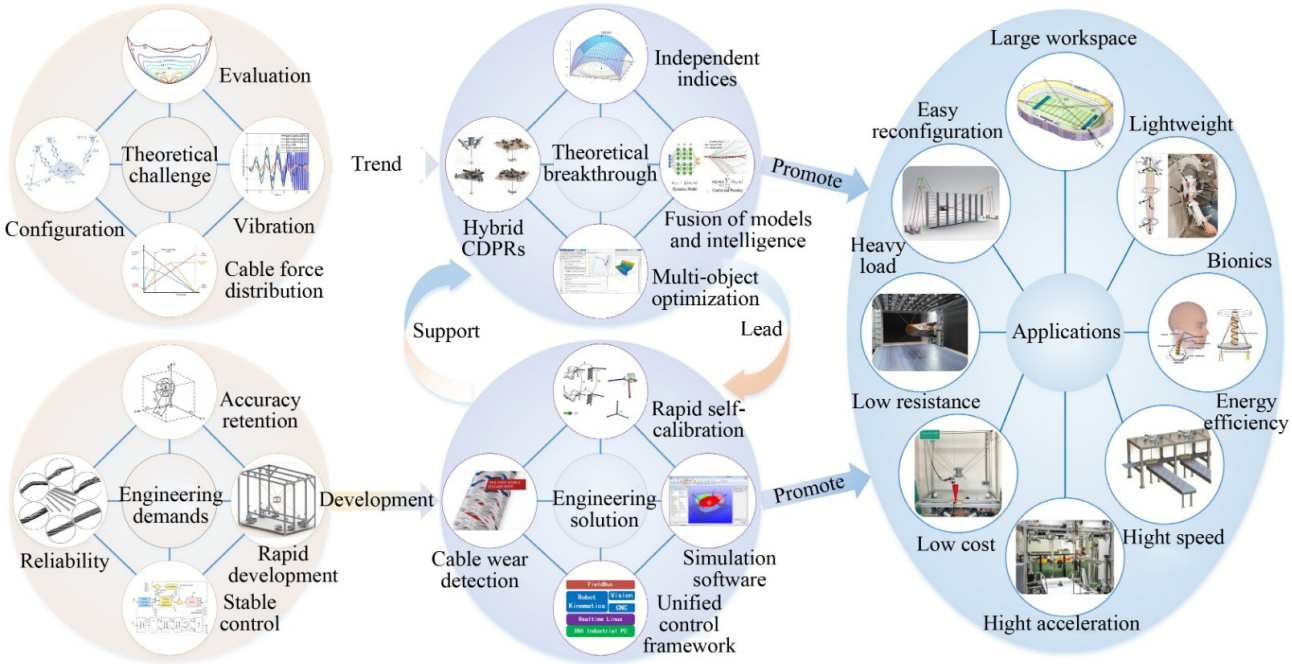

Fig. 15 Research and application prospects of CDPRs.

when adopted in the control. Because terminal accuracy is frequently the most important parameter of a robot, kinematics-based control is widely used in CDPRs. Elastostatic and dynamic models are adopted to improve performance. Comprehensive optimization (co-optimization) of the configuration design and control, as well as the fusion of models and intelligent algorithms, will be expected to further improve the performance of the CDPRs.

In terms of application, CDPRs have been successfully used in the fields of astronomical telescopes, lifting and handling, motion simulators, rehabilitation, and bionics. CDPRs will be promoted in more fields in the future with a solid industrial foundation, and the following challenges require consideration.

1) The reliability and service life of CDPRs. The CDPR cables easily wear and break during operation, and it is difficult to guarantee the sustainable and reliable operating time of the CDPRs. There is a lack of relevant research and specifications for the durability of CDPRs, such as cable wear detection and replacement specifications. The Liebherr Corporation has conducted related research and proposed vision-based cable wear detection [208].

2) The accuracy retention of CDPRs. Owing to factors such as the reconfiguration, nonlinear deformation of cables, and creep of cables under long-term tension, it is difficult to guarantee the accuracy retention of CDPRs. Accuracy degradation has an important impact on their application, particularly in industrial applications. Rapid self-calibration is a feasible approach.

3) The vibrations control of CDPRs. CDPRs are prone to vibration owing to cable flexibility and low rigidity. Although various vibration suppression methods have been proposed for CDPRs, they are often specific and lack versatility for different types of CDPRs. In actual implementations of vibration suppression controls, the performance of the controller is usually excessively required, resulting in high cost. A unified framework for the control hardware and software should be proposed.

4) The rapid development cycle of CDPRs. On one hand, the industrial infrastructure of CDPRs is still insufficient, such as high-performance cables, drive modules, and control systems. On the other hand, there is a lack of mature software that supports the efficient analysis and development of CDPRs. The software CASPR developed by Lau et al. [209] and WireX developed by Pott [210] have been good attempts, but continuous improvement is still required.

Nomenclature

Abbreviations

3D	Three dimensional
AFI	Average force index
CDPR	Cable-driven parallel robot
CSPR	Cable-suspended parallel robot
CSS	Constant stiffness space
DFW	Dynamic feasible workspace
DOF	Degree-of-freedom
FAST	Five-hundred-meter Aperture Spherical radio Telescope

FCW	Force closure workspace
FEM	Finite element method
FFW	Force feasible workspace
LPV	Linear parameter-varying
MFI	Maximum force index
P, R, T	Prismatic, rotation, translation joints, respectively
PID	Proportional-integral-derivative
VSD	Variable stiffness device
WCW	Wrench closure workspace
WFW	Wrench feasible workspace

Variables

A_i	Cross-sectional area of the ith cable
$\boldsymbol{a}_i$	Position of cable outlet point A_i on the base
$\boldsymbol{b}_i$	Position of the cable connection point B_i in the local coordinate system
E_i	Elastic modulus of the ith cable
$\boldsymbol{f}_{ik}(\boldsymbol{p},\boldsymbol{a})$	Inverse kinematics of the CDPR
$\boldsymbol{F}$	External force acting on the end effector
$\boldsymbol{G}(\boldsymbol{T})$	Target function for cable force optimization
$\boldsymbol{H}$	Hessian matrix
$\boldsymbol{I}$	Unit matrix
$\boldsymbol{J}$	Structure matrix of the CDPR
$\boldsymbol{J}^+$	Moore–Penrose inverse of matrix $\boldsymbol{J}$
$\boldsymbol{K}$	Stiffness matrix of the CDPR
$\boldsymbol{K}_1$	Geometric stiffness matrix or the active stiffness
$\boldsymbol{K}_2$	Cable stiffness matrix or the passive stiffness
l_i	Length of the ith cable
$\boldsymbol{L}$	Vector of cable lengths
m	Numbers of driving cables
$\boldsymbol{M}$	External torque acting on the end effector
n	Number of terminal DOFs
p	Order of the norm
$\boldsymbol{p}$	Position of the end effector
${}^{O}\boldsymbol{R}_p$	Rotation matrix of the end effector frame $\{P\text{–}xyz\}$ with respect to the base frame $\{O\text{–}XYZ\}$
t_i	Amplitude of the tension on the ith cable
$t_{\min}$, $t_{\max}$	Minimum and maximum limits of the cable-force range, respectively
$t_{\mathrm{ref},i}$	Target cable force of the ith cable
$\boldsymbol{T}$	Cable-force vector of the CDPR
$\boldsymbol{u}_i$	Unit directional vector of the ith cable
$\boldsymbol{W}$	External wrench acting on the end effector
$\boldsymbol{X}$	Motion of the end effector
λ	Arbitrary vector of n-dimension

Acknowledgements This work was supported in part by the National Natural Science Foundation of China (Grant Nos. 52105025 and U19A20101). The authors would like to thank the National Institute of Standards and Technology, JASO Industrial Cranes, Max Planck Institute for Biological Cybernetics, Institute for Fluid Dynamics and Ship Theory at the Hamburg University of Technology, and ONERA for providing and giving the permission to use some of the figures in the paper. The authors would also like to thank the editors and reviewers for their pertinent comments and suggestions.

Open Access This article is licensed under a Creative Commons Attribution 4.0 International License, which permits use, sharing, adaptation, distribution, and reproduction in any medium or format as long as appropriate credit is given to the original author(s) and source, a link to the Creative Commons license is provided, and the changes made are indicated.

The images or other third-party material in this article are included in the article's Creative Commons license, unless indicated otherwise in a credit line to the material. If material is not included in the article's Creative Commons license and your intended use is not permitted by statutory regulation or exceeds the permitted use, you will need to obtain permission directly from the copyright holder.

Visit http://creativecommons.org/licenses/by/4.0/ to view a copy of this license.

References

1. Gough V, Whitehall S G. Universal tyre test machine. In: Proceedings of the 9th International Congress FISITA. London, 1962, 117–137
2. Stewart D. A platform with six degrees of freedom. Proceedings of the Institution of Mechanical Engineers, 1965, 180(1): 371–386
3. Shao Z F, Tang X Q, Chen X, Wang L P. Research on the inertia matching of the Stewart parallel manipulator. Robotics and Computer-Integrated Manufacturing, 2012, 28(6): 649–659
4. Zhang Z K, Wang L P, Shao Z F. Improving the kinematic performance of a planar 3-RRR parallel manipulator through actuation mode conversion. Mechanism and Machine Theory, 2018, 130: 86–108
5. Staicu S, Shao Z F, Zhang Z K, Tang X Q, Wang L P. Kinematic analysis of the X4 translational–rotational parallel robot. International Journal of Advanced Robotic Systems, 2018, 15(5): 1729881418803849
6. Wang D, Wang L P, Wu J, Ye H. An experimental study on the dynamics calibration of a 3-DOF parallel tool head. IEEE/ASME Transactions on Mechatronics, 2019, 24(6): 2931–2941
7. Dong W, Du Z J, Xiao Y Q, Chen X G. Development of a parallel kinematic motion simulator platform. Mechatronics, 2013, 23(1): 154–161
8. Clavel R. DELTA: a fast robot with parallel geometry. In: Proceedings of the 18th International Symposium on Industrial Robots. New York: Springer, 1988, 91–100
9. Chen X, Liu X J, Xie F G, Sun T. A comparison study on motion/force transmissibility of two typical 3-DOF parallel manipulators: the sprint Z3 and A3 tool heads. International Journal of Advanced Robotic Systems, 2014, 11(1): 5
10. Gosselin C. Cable-driven parallel mechanisms: state of the art and perspectives. Mechanical Engineering Reviews, 2014, 1(1): DSM0004

11. Landsberger S E. Design and construction of a cable-controlled, parallel link manipulator. Dissertation for the Doctoral Degree. Cambridge: Massachusetts Institute of Technology, 1984
12. Tanaka M, Seguchi Y, Shimada S. Kinemato-statics of SkyCam-type wire transport system. In: Proceedings of USA-Japan Symposium on Flexible Automation, Crossing Bridges: Advances in Flexible Automation and Robotics. Minneapolis Minnesota: The Society, 1988, 689–694
13. Albus J, Bostelman R, Dagalakis N. The NIST robocrane. Journal of Robotic Systems, 1993, 10(5): 709–724
14. NIST. Schematics: TensileTruss Robotic System and NIST's RoboCrane. Available from NIST website, 2021
15. NIST. Gantries. Available from NIST website, 2017
16. NIST. Wide View: RoboCrane® for Aircraft Maintenance. Available from NIST website, 2006
17. NIST. Material Handling. Available from NIST website, 2017
18. NIST. Robocrane: large scale manufacturing using cable control. Available from NIST website, 2021
19. Wikipedia. RoboCrane. Available from Wikipedia website, 2021
20. Qian L, Yao R, Sun J H, Xu J L, Pan Z C, Jiang P. FAST: its scientific achievements and prospects. The Innovation, 2020, 1(3): 100053
21. Tang X Q, Shao Z F. Trajectory generation and tracking control of a multi-level hybrid support manipulator in FAST. Mechatronics, 2013, 23(8): 1113–1122
22. El-Ghazaly G, Gouttefarde M, Creuze V. Adaptive terminal sliding mode control of a redundantly-actuated cable-driven parallel manipulator: CoGiRo. In: Pott A, Bruckmann T, eds. Cable-Driven Parallel Robots. Cham: Springer, 2014, 32: 179–200
23. JASO Industrial. CraneBot: the flexible robotic crane. Available from JASO Industrial website, 2022
24. Wu Y L, Cheng H H, Fingrut A, Crolla K, Yam Y, Lau D. CU-brick cable-driven robot for automated construction of complex brick structures: from simulation to hardware realization. In: Proceedings of 2018 IEEE International Conference on Simulation, Modeling, and Programming for Autonomous Robots (SIMPAR). Brisbane: IEEE, 2018, 166–173
25. Bruckmann T. Reichert C, Meik M, Lemmen P, Spengler A, Mattern H, König M. Concept studies of automated construction using cable-driven parallel robots. In: Gosselin C, Cardou P, Bruckmann T, Pott A, eds. Cable-Driven Parallel Robots. Cham: Springer, 2018, 53: 364–375
26. Hephaestus. About the project. Available from Hephaestus website, 2017
27. Pan W, Iturralde K, Bock T, Martinez R G, Juez O M, Finocchiaro P. A Conceptual Design of an Integrated Façade System to Reduce Embodied Energy in Residential Buildings. Sustainability, 2020, 12(14): 5730
28. Bruckmann T, Sturm C, Fehlberg L, Reichert C. An energy-efficient wire-based storage and retrieval system. In: Proceedings of 2013 IEEE/ASME International Conference on Advanced Intelligent Mechatronics. Wollongong: IEEE, 2013, 631–636
29. Miermeister P, Lächele M, Boss R, Masone C, Schenk C, Tesch J, Kerger M, Teufel H, Pott A, Bülthoff H H. The cablerobot simulator large scale motion platform based on cable robot technology. In: Proceedings of 2016 IEEE/RSJ International Conference on Intelligent Robots and Systems (IROS). Daejeon: IEEE, 2016, 3024–3029
30. Bruckmann T, Mikelsons L, Brandt T, Schramm D, Pott A, Abdel-Maksoud M. A novel tensed mechanism for simulation of maneuvers in wind tunnels. In: Proceedings of the ASME 2009 International Design Engineering Technical Conferences and Computers and Information in Engineering Conference. San Diego: ASME, 2009, 17–24
31. Farcy D, Llibre M, Carton P, Lambert C. SACSO: wire-driven parallel set-up for dynamic tests in wind tunnel–review of principles and advantages for identification of aerodynamic models for flight mechanics. In: Proceedings of the 8th ONERA-DLR Aerospace Symposium. Göttingen, 2007
32. Barnett E, Gosselin C. Large-scale 3D printing with a cable-suspended robot. Additive Manufacturing, 2015, 7: 27–44
33. Zi B, Wang N, Qian S, Bao K L. Design, stiffness analysis and experimental study of a cable-driven parallel 3D printer. Mechanism and Machine Theory, 2019, 132: 207–222
34. Qian S, Bao K L, Zi B, Wang N. Kinematic calibration of a cable-driven parallel robot for 3D printing. Sensors, 2018, 18(9): 2898
35. Pott A, Tempel P, Verl A, Wulle F. Design, implementation and long-term running experiences of the cable-driven parallel robot CaRo printer. In: Pott A, Bruckmann T, eds. CableCon 2019: Cable-Driven Parallel Robots. Cham: Springer, 2019, 74: 379–390
36. Masiero S, Celia A, Armani M, Rosati G. A novel robot device in rehabilitation of post-stroke hemiplegic upper limbs. Aging clinical and experimental research, 2006, 18(6): 531–535
37. Surdilovic D, Bernhardt R. STRING-MAN: a new wire robot for gait rehabilitation. In: Proceedings of IEEE International Conference on Robotics and Automation. New Orleans: IEEE, 2004, 2031–2036
38. Surdilovic D, Bernhardt R, Schmidt T, Zhang J. 26 STRING-MAN: A novel wire robot for gait rehabilitation. In: Bien Z Z, Stefanov D, eds. Advances in Rehabilitation Robotics. Lecture Notes in Control and Information Science. Berlin, Heidelberg: Springer, 2006, 306: 413–424
39. Mao Y, Agrawal S K. Design of a cable-driven arm exoskeleton (CAREX) for neural rehabilitation. IEEE Transactions on Robotics, 2012, 28(4): 922–931
40. Mao Y, Jin X, Gera Dutta G, Scholz J P, Agrawal S K. Human movement training with a cable driven ARm EXoskeleton (CAREX). IEEE Transactions on Neural Systems and Rehabilitation Engineering, 2015, 23(1): 84–92
41. Ming A, Higuchi T. Study on multiple degree-of-freedom positioning mechanism using wires. I: concept, design and control. International Journal of the Japan Society for Precision Engineering, 1994, 28(2): 131–138
42. Nguyen V D. Constructing force-closure grasps. The International Journal of Robotics Research, 1988, 7(3): 3–16
43. Verhoeven R. Analysis of the workspace of tendon-based Stewart platforms. Dissertation for the Doctoral Degree. Essen: University of Duisburg-Essen, 2004
44. Riechel A T, Bosscher P, Lipkin H, Ebert-Uphoff I. Concept

paper: cable-driven robots for use in hazardous environments. In: Proceedings of the 10th International Topical Meeting on Robotics and Remote Systems for Hazardous Environments. Gainesville, 2004

45. Kawamura S, Kino H, Won C. High-speed manipulation by using parallel wire-driven robots. Robotica, 2000, 18(1): 13–21
46. Roberts R G, Graham T, Lippitt T. On the inverse kinematics, statics, and fault tolerance of cable-suspended robots. Journal of Robotic Systems, 1998, 15(10): 581–597
47. Seon J A, Park S, Ko S Y, Park J O. Cable configuration analysis to increase the rotational range of suspended 6-DOF cable driven parallel robots. In: Proceedings of 2016 the 16th International Conference on Control, Automation and Systems (ICCAS). Gyeongju: IEEE, 2016, 1047–1052
48. Wang W F. Research on redundantly restrained cable-driven parallel mechanism for simulating force. Dissertation for the Doctoral Degree. Beijing: Tsinghua University, 2016
49. Eden J, Song C, Tan Y, Oetomo D, Lau D. CASPR-ROS: a generalised cable robot software in ROS for hardware. In: Gosselin C, Cardou P, Bruckmann T, Pott A, eds. Cable-Driven Parallel Robots. Mechanisms and Machine Science. Cham: Springer, 2018, 53: 50–61
50. Gao B T, Zhu Z Y, Zhao J G, Jiang L J. Inverse kinematics and workspace analysis of a 3 DOF flexible parallel humanoid neck robot. Journal of Intelligent & Robotic Systems, 2017, 87(2): 211–229
51. Zhang Z K, Shao Z F, Wang L P. Optimization and implementation of a high-speed 3-DOFs translational cable-driven parallel robot. Mechanism and Machine Theory, 2020, 145: 103693
52. Lau D, Oetomo D, Halgamuge S K. Generalized modeling of multilink cable-driven manipulators with arbitrary routing using the cable-routing matrix. IEEE Transactions on Robotics, 2013, 29(5): 1102–1113
53. Rone W S, Saab W, Ben-Tzvi P. Design, modeling, and integration of a flexible universal spatial robotic tail. Journal of Mechanisms and Robotics, 2018, 10(4): 041001
54. Li C S, Gu X Y, Ren H L. A cable-driven flexible robotic grasper with Lego-like modular and reconfigurable joints. IEEE/ASME Transactions on Mechatronics, 2017, 22(6): 2757–2767
55. Landsberger S E, Sheridan T B. A new design for parallel link manipulator. In: Proceedings of 1985 IEEE International Conference on Systems. Tucson: IEEE, 1985, 812–814
56. Dekker R, Khajepour A, Behzadipour S. Design and testing of an ultra-high-speed cable robot. International Journal of Robotics and Automation, 2006, 21(1): 25–34
57. Behzadipour S, Khajepour A. A new cable-based parallel robot with three degrees of freedom. Multibody System Dynamics, 2005, 13(4): 371–383
58. Zhang Z K, Shao Z F, Wang L P, Shih A J. Optimal design of a high-speed pick-and-place cable-driven parallel robot. In: Gosselin C, Cardou P, Bruckmann T, Pott A, eds. Cable-Driven Parallel Robots. Cham: Springer, 2018, 340–352
59. Duan Q J, Vashista V, Agrawal S K. Effect on wrench-feasible workspace of cable-driven parallel robots by adding springs. Mechanism and Machine Theory, 2015, 86: 201–210
60. Taghavi A, Behzadipour S, Khalilinasab N, Zohoor H. Workspace improvement of two-link cable-driven mechanisms with spring cable. In: Bruckmann T, Pott A, eds. Cable-Driven Parallel Robots. Berlin, Heidelberg: Springer, 2013, 201–213
61. von Zitzewitz J, Fehlberg L, Bruckmann T, Vallery H. Use of passively guided deflection units and energy-storing elements to increase the application range of wire robots. In: Bruckmann T, Pott A, eds. Cable-Driven Parallel Robots. Berlin, Heidelberg: Springer, 2013, 167–184
62. Xie G Q, Zhang Z K, Shao Z F, Wang L P. Research on the orientation error of the translational cable-driven parallel robots. Journal of Mechanisms and Robotics, 2022, 14(3): 031003
63. Bosscher P, Williams R L II, Tummino M. A concept for rapidly-deployable cable robot search and rescue systems. In: Proceedings of the ASME 2005 International Design Engineering Technical Conferences and Computers and Information in Engineering Conference. California: ASME, 2005, 589–598
64. Alikhani A, Behzadipour S, Alasty A, Sadough Vanini S A. Design of a large-scale cable-driven robot with translational motion. Robotics and Computer-Integrated Manufacturing, 2011, 27(2): 357–366
65. Gagliardini L, Caro S, Gouttefarde M, Girin A. Discrete reconfiguration planning for cable-driven parallel robots. Mechanism and Machine Theory, 2016, 100: 313–337
66. Wang H B, Kinugawa J, Kosuge K. Exact kinematic modeling and identification of reconfigurable cable-driven robots with dual-pulley cable guiding mechanisms. IEEE/ASME Transactions on Mechatronics, 2019, 24(2): 774–784
67. Pott A. Cable-Driven Parallel Robots: Theory and Application. Cham: Springer, 2018
68. Gonzalez-Rodriguez A, Castillo-Garcia F J, Ottaviano E, Rea P, Gonzalez-Rodriguez A G. On the effects of the design of cable-driven robots on kinematics and dynamics models accuracy. Mechatronics, 2017, 43: 18–27
69. Jin X J, Jung J, Piao J L, Choi E, Park J O, Kim C S. Solving the pulley inclusion problem for a cable-driven parallel robotic system: extended kinematics and twin-pulley mechanism. Journal of Mechanical Science and Technology, 2018, 32(6): 2829–2838
70. Idà E, Bruckmann T, Carricato M. Rest-to-rest trajectory planning for underactuated cable-driven parallel robots. IEEE Transactions on Robotics, 2019, 35(6): 1338–1351
71. Zhang Z K, Xie G Q, Shao Z F, Gosselin C. Kinematic calibration of cable-driven parallel robots considering the pulley kinematics. Mechanism and Machine Theory, 2022, 169: 104648
72. Pott A. Influence of pulley kinematics on cable-driven parallel robots. In: Lenarcic J, Husty M, eds. Latest Advances in Robot Kinematics. Dordrecht: Springer, 2012, 197–204
73. Schmidt V, Pott A. Implementing extended kinematics of a cable-driven parallel robot in real-time. In: Bruckmann T, Pott A, eds. Cable-Driven Parallel Robots. Berlin: Springer, 2013, 287–298
74. Kozak K, Zhou Q, Wang J S. Static analysis of cable-driven manipulators with non-negligible cable mass. IEEE Transactions on Robotics, 2006, 22(3): 425–433
75. Yao R, Tang X Q, Li T M, Ren G X. Analysis and design of 3T cable-driven parallel manipulator for the feedback's orientation of the large radio telescope. Journal of Mechanical Engineering,

2007, 43(11): 105–109 (in Chinese)
76. Tang X Q, Shao Z F, Yao R. Research and application of cable-drive parallel mechanism and rigid parallel mechanism—research and development of the feed support system of the 40 m scale model of FAST. Beijing: Tsinghua University Press, 2020
77. Fang S Q. Design, modeling and motion control of tendon-based parallel manipulators. Dissertation for the Doctoral Degree. Essen: University of Duisburg-Essen, 2005
78. Merlet J P. Kinematics of the wire-driven parallel robot MARIONET using linear actuators. In: Proceedings of 2008 IEEE International Conference on Robotics and Automation. Pasadena: IEEE, 2008, 3857–3862
79. Aref M M, Oftadeh R, Taghirad H D. Kinematics and Jacobian analysis of the KNTU CDRPM: a cable driven redundant parallel manipulator. In: Proceedings of the 17th Iranian Conference on Electrical Engineering. Tehran, 2009, 319–324
80. Fabritius M, Pott A. A forward kinematic code for cable-driven parallel robots considering cable sagging and pulleys. In: Lenarčič J, Siciliano B, eds. Advances in Robot Kinematics 2020. ARK 2020. Springer Proceedings in Advanced Robotics. Cham: Springer, 2021, 15: 218–225
81. Santos J C, Gouttefarde M. A real-time capable forward kinematics algorithm for cable-driven parallel robots considering pulley kinematics. In: Lenarčič J, Siciliano B, eds. Advances in Robot Kinematics 2020. ARK 2020. Springer Proceedings in Advanced Robotics. Cham: Springer, 2021, 15: 199–208
82. Hassan M, Khajepour A. Optimization of actuator forces in cable-based parallel manipulators using convex analysis. IEEE Transactions on Robotics, 2008, 24(3): 736–740
83. Borgstrom P H, Jordan B L, Borgstrom B J, Stealey M J, Sukhatme G S, Batalin M A, Kaiser W J. NIMS-PL: a cable-driven robot with self-calibration capabilities. IEEE Transactions on Robotics, 2009, 25(5): 1005–1015
84. Bruckmann T, Pott A, Franitza D, Hiller M. A modular controller for redundantly actuated tendon-based Stewart platforms. In: Proceedings of European Conference on Mechanism Science. Obergurgl, 2006, 1–12
85. Notash L. Designing positive tension for wire-actuated parallel manipulators. In: Kumar V, Schmiedeler J, Sreenivasan S, Su H J, eds. Advances in Mechanisms, Robotics and Design Education and Research. Heidelberg: Springer, 2013, 14: 251–263
86. Gosselin C, Grenier M. On the determination of the force distribution in overconstrained cable-driven parallel mechanisms. Meccanica, 2011, 46(1): 3–15
87. Pott A, Bruckmann T, Mikelsons L. Closed-form force distribution for parallel wire robots. In: Kecskeméthy A, Müller A, eds. Computational Kinematics. Berlin: Springer, 2009, 25–34
88. Lim W B, Yeo S H, Yang G L. Optimization of tension distribution for cable-driven manipulators using tension-level index. IEEE/ASME Transactions on Mechatronics, 2014, 19(2): 676–683
89. Mikelsons L, Bruckmann T, Hiller M, Schramm D. A real-time capable force calculation algorithm for redundant tendon-based parallel manipulators. In: Proceedings of IEEE International Conference on Robotics and Automation. Pasadena: IEEE, 2008, 3869–3874
90. Taghirad H D, Bedoustani Y B. An analytic-iterative redundancy resolution scheme for cable-driven redundant parallel manipulators. IEEE Transactions on Robotics, 2011, 27(6): 1137–1143
91. Yang K S, Yang G L, Wang Y, Zhang C, Chen S L. Stiffness-oriented cable tension distribution algorithm for a 3-DOF cable-driven variable-stiffness module. In: Proceedings of IEEE International Conference on Advanced Intelligent Mechatronics. Munich: IEEE, 2017, 454–459
92. Azizian K, Cardou P, Moore B. Classifying the boundaries of the wrench-closure workspace of planar parallel cable-driven mechanisms by visual inspection. Journal of Mechanisms and Robotics, 2012, 4(2): 024503
93. Bruckmann T, Pott A, Hiller M. Calculating force distributions for redundantly actuated tendon-based Stewart platforms. In: Lennarčič J, Roth B, eds. Advances in Robot Kinematics. Dordrecht: Springer, 2006, 403–412
94. Gouttefarde M, Lamaury J, Reichert C, Bruckmann T. A versatile tension distribution algorithm for n-DOF parallel robots driven by n+2 cables. IEEE Transactions on Robotics, 2015, 31(6): 1444–1457
95. Rasheed T, Long P, Marquez-Gamez D, Caro S. Tension distribution algorithm for planar mobile cable-driven parallel robots. In: Gosselin C, Cardou P, Bruckmann T, Pott A, eds. Cable-Driven Parallel Robots. Cham: Springer, 2018, 53: 268–279
96. Cui Z W, Tang X Q, Hou S H, Sun H N. Non-iterative geometric method for cable-tension optimization of cable-driven parallel robots with 2 redundant cables. Mechatronics, 2019, 59: 49–60
97. Alp A B, Agrawal S K. Cable suspended robots: design, planning and control. In: Proceedings of 2002 IEEE International Conference on Robotics and Automation. Washington: IEEE, 2002, 4: 4275–4280
98. Gouttefarde M, Gosselin C M. Analysis of the wrench-closure workspace of planar parallel cable-driven mechanisms. IEEE Transactions on Robotics, 2006, 22(3): 434–445
99. Pham C B, Yeo S H, Yang G L, Kurbanhusen M S, Chen I M. Force-closure workspace analysis of cable-driven parallel mechanisms. Mechanism and Machine Theory, 2006, 41(1): 53–69
100. Ebert-Uphoff I, Voglewede P A. On the connection between cable-driven robots, parallel manipulators and grasping. In: Proceedings of 2004 IEEE International Conference on Robotics & Automation. New Orleans: IEEE, 2004, 4521–4526
101. Bosscher P, Riechel A T, Ebert-Uphoff I. Wrench-feasible workspace generation for cable-driven robots. IEEE Transactions on Robotics, 2006, 22(5): 890–902
102. Riechel A T, Ebert-Uphoff I. Force-feasible workspace analysis for underconstrained, point-mass cable robots. In: Proceedings of 2004 IEEE International Conference on Robotics and Automation. New Orleans: IEEE, 2004, 4956–4962
103. Verhoeven R, Hiller M. Estimating the controllable workspace of tendon-based Stewart platforms. In: Lenarčič J, Stanišić M M, eds. Advances in Robot Kinematics. Dordrecht: Springer, 2000, 277–284
104. Alikhani A, Behzadipour S, Sadough Vanini S A, Alasty A.

Workspace analysis of a three DOF cable-driven mechanism. Journal of Mechanisms and Robotics, 2009, 1(4): 041005
105. Barrette G, Gosselin C M. Determination of the dynamic workspace of cable-driven planar parallel mechanisms. Journal of Mechanical Design, 2005, 127(2): 242–248
106. Gagliardini L, Gouttefarde M, Caro S. Determination of a dynamic feasible workspace for cable-driven parallel robots. In: Lenarčič J, Merlet J P, eds. Advances in Robot Kinematics 2016. Springer Proceedings in Advanced Robotics. Cham: Springer, 2018, 4: 361–370
107. Shao Z F, Peng F Z, Zhang Z K, Li H S. Research on the dynamic trajectory of cable-suspended parallel robot considering the uniformity of cable tension. In: Proceedings of 2019 IEEE the 9th Annual International Conference on CYBER Technology in Automation, Control, and Intelligent Systems (CYBER). Suzhou: IEEE, 2019, 795–801
108. Zhang Y J, Zhang Y R, Dai X W, Yang Y. Workspace analysis of a novel 6-DOF cable-driven parallel robot. In: Proceedings of 2009 IEEE International Conference on Robotics and Biomimetics (ROBIO). Guilin: IEEE, 2009, 2403–2408
109. Zlatanov D, Agrawal S, Gosselin C M. Convex cones in screw spaces. Mechanism and Machine Theory, 2005, 40(6): 710–727
110. Dong X D, Duan Q J, Ma B, Duan X C. Workspace algorithm of cable-driven serial and parallel manipulators based on convex set theory. China Mechanical Engineering, 2016, 27(18): 2424–2429, 2436 (in Chinese)
111. Gouttefarde M, Daney D, Merlet J P. Interval-analysis-based determination of the wrench-feasible workspace of parallel cable-driven robots. IEEE Transactions on Robotics, 2011, 27(1): 1–13
112. Abbasnejad G, Eden J, Lau D. Generalized ray-based lattice generation and graph representation of wrench-closure workspace for arbitrary cable-driven robots. IEEE Transactions on Robotics, 2019, 35(1): 147–161
113. Jiang X L, Barnett E, Gosselin C. Periodic trajectory planning beyond the static workspace for 6-DOF cable-suspended parallel robots. IEEE Transactions on Robotics, 2018, 34(4): 1128–1140
114. Jiang X L, Gosselin C. Dynamic point-to-point trajectory planning of a three-DOF cable-suspended parallel robot. IEEE Transactions on Robotics, 2016, 32(6): 1550–1557
115. Dion-Gauvin P, Gosselin C. Trajectory planning for the static to dynamic transition of point-mass cable-suspended parallel mechanisms. Mechanism and Machine Theory, 2017, 113: 158–178
116. Gosselin C, Ren P, Foucault S. Dynamic trajectory planning of a two-DOF cable-suspended parallel robot. In: Proceedings of 2012 IEEE International Conference on Robotics and Automation (ICRA). Saint Paul: IEEE, 2012, 1476–1481
117. Gosselin C. Global planning of dynamically feasible trajectories for three-DOF spatial cable-suspended parallel robots. In: Bruckmann T, Pott A, eds. Cable-Driven Parallel Robots. Berlin: Springer, 2013, 3–22
118. Voglewede P A, Ebert-Uphoff I. Application of the antipodal grasp theorem to cable driven robots. IEEE Transactions on Robotics, 2005, 21(4): 713–718
119. Behzadipour S, Khajepour A. Stiffness of cable-based parallel manipulators with application to stability analysis. Journal of Mechanical Design, 2006, 128(1): 303–310
120. Surdilovic D, Radojicic J, Krüger J. Geometric stiffness analysis of wire robots: a mechanical approach. In: Bruckmann T, Pott A, eds. Cable-Driven Parallel Robots. Berlin, Heidelberg: Springer, 2013, 389–404
121. Simaan N, Shoham M. Geometric interpretation of the derivatives of parallel robots' Jacobian matrix with application to stiffness control. Journal of Mechanical Design, 2003, 125(1): 33–42
122. Cui Z W, Tang X Q, Hou S H, Sun H N. Research on controllable stiffness of redundant cable-driven parallel robots. IEEE/ASME Transactions on Mechatronics, 2018, 23(5): 2390–2401
123. Yeo S H, Yang G, Lim W B. Design and analysis of cable-driven manipulators with variable stiffness. Mechanism and Machine Theory, 2013, 69: 230–244
124. Jamshidifar H, Khajepour A, Fidan B, Rushton M. Kinematically-constrained redundant cable-driven parallel robots: modeling, redundancy analysis, and stiffness optimization. IEEE/ASME Transactions on Mechatronics, 2017, 22(2): 921–930
125. Bolboli J, Khosravi M A, Abdollahi F. Stiffness feasible workspace of cable-driven parallel robots with application to optimal design of a planar cable robot. Robotics and Autonomous Systems, 2019, 114: 19–28
126. Cui Z W, Tang X Q, Hou S H, Sun H N, Wang D J. Calculation and analysis of constant stiffness space for redundant cable-driven parallel robots. IEEE Access, 2019, 7: 75407–75419
127. Alamdari A, Haghighi R, Krovi V. Stiffness modulation in an elastic articulated-cable leg-orthosis emulator: theory and experiment. IEEE Transactions on Robotics, 2018, 34(5): 1266–1279
128. Yang K S, Yang G L, Chen S L, Wang Y, Zhang C, Fang Z J, Zheng T J, Wang C C. Study on stiffness-oriented cable tension distribution for a symmetrical cable-driven mechanism. Symmetry, 2019, 11(9): 1158
129. Du J L, Bao H, Cui C Z. Stiffness and dexterous performances optimization of large workspace cable-driven parallel manipulators. Advanced Robotics, 2014, 28(3): 187–196
130. Yuan H, Courteille E, Deblaise D. Static and dynamic stiffness analyses of cable-driven parallel robots with non-negligible cable mass and elasticity. Mechanism and Machine Theory, 2015, 85: 64–81
131. Arsenault M. Workspace and stiffness analysis of a three-degree-of-freedom spatial cable-suspended parallel mechanism while considering cable mass. Mechanism and Machine Theory, 2013, 66: 1–13
132. Azizian K, Cardou P. The dimensional synthesis of spatial cable-driven parallel mechanisms. Journal of Mechanisms and Robotics, 2013, 5(4): 044502
133. Abbasnejad G, Yoon J, Lee H. Optimum kinematic design of a planar cable-driven parallel robot with wrench-closure gait trajectory. Mechanism and Machine Theory, 2016, 99: 1–18
134. Song D, Zhang L X, Xue F. Configuration optimization and a tension distribution algorithm for cable-driven parallel robots. IEEE Access, 2018, 6: 33928–33940
135. Zi B, Yin G C, Zhang D. Design and optimization of a hybrid-driven waist rehabilitation robot. Sensors, 2016, 16(12): 2121

136. Xu L, Cao Y, Chen J, Jiang S. Design and workspace optimization of a 6/6 cable-suspended parallel robot. In: Proceedings of 2010 International Conference on Computer Application and System Modeling (ICCASM 2010). Taiyuan: IEEE, 2010, 10: 610–614
137. Hernandez E, Valdez S I, Carbone G, Ceccarelli M. Design optimization of a cable-driven parallel robot in upper arm training-rehabilitation processes. In: Carvalho J C M, Martins D, Simoni R, Simas H, eds. Multibody Mechatronic Systems. Cham: Springer, 2018, 413–423
138. Yang G L, Pham C B, Yeo S H. Workspace performance optimization of fully restrained cable-driven parallel manipulators. In: Proceedings of 2006 IEEE/RSJ International Conference on Intelligent Robots and Systems. Beijing: IEEE, 2006, 85–90
139. Duan Q J, Li Q H, Li F, Duan X C. Analysis of the workspace of the cable-spring mechanism. Journal of Mechanical Engineering, 2016, 52(15): 15–20
140. Tang X, Tang L, Wang J, Sun D. Workspace quality analysis and application for a completely restrained 3-DOF planar cable-driven parallel manipulator. Journal of Mechanical Science and Technology, 2013, 27(8): 2391–2399
141. Newman M, Zygielbaum A, Terry B. Static analysis and dimensional optimization of a cable-driven parallel robot. In: Gosselin C, Cardou P, Bruckmann T, Pott A, eds. Cable-Driven Parallel Robots. Cham: Springer, 2018, 152–166
142. Hanafie J, Nurahmi L, Caro S, Pramujati B. Design optimization of spatial four cables suspended cable driven parallel robot for rapid life-scan. AIP Conference Proceedings, 2018, 1983(1): 060007
143. Laribi M A, Carbone G, Zeghloul S. On the optimal design of cable-driven parallel robot with a prescribed workspace for upper limb rehabilitation tasks. Journal of Bionics Engineering, 2019, 16(3): 503–513
144. Ennaiem F, Chaker A, Arévalo J S S, Laribi M A, Bennour S, Mlika A, Romdhane L, Zeghloul S. Optimal design of a rehabilitation four cable-driven parallel robot for daily living activities. In: Zeghloul S, Laribi M A, Sandoval Arevalo J S, eds. Advances in Service and Industrial Robotics. Cham: Springer, 2020, 3–12
145. Bryson J T, Jin X, Agrawal S K. Optimal design of cable-driven manipulators using particle swarm optimization. Journal of Mechanisms and Robotics, 2016, 8(4): 041003
146. Shao Z F, Tang X Q, Yi W M. Optimal design of a 3-DOF cable-driven upper arm exoskeleton. Advances in Mechanical Engineering, 2014, 6: 157096
147. Yao R, Tang X Q, Wang J S, Huang P. Dimensional optimization design of the four-cable-driven parallel manipulator in fast. IEEE/ASME Transactions on Mechatronics, 2010, 15(6): 932–941
148. Gueners D, Chanal H, Bouzgarrou B C. Stiffness optimization of a cable driven parallel robot for additive manufacturing. In: Proceedings of 2020 IEEE International Conference on Robotics and Automation (ICRA). Paris: IEEE, 2020, 843–849
149. Torres-Mendez S, Khajepour A. Design optimization of a warehousing cable-based robot. In: Proceedings of International Design Engineering Technical Conferences and Computers and Information in Engineering Conference. Buffalo: ASME, 2014, V05AT08A091
150. Li Y M, Xu Q S. GA-based multi-objective optimal design of a planar 3-DOF cable-driven parallel manipulator. In: Proceedings of 2006 IEEE International Conference on Robotics and Biomimetics. Kunming: IEEE, 2006, 1360–1365
151. Cui Z W, Tang X Q, Hou S H, Sun H N, Wang D J. Optimization design of redundant cable driven parallel robots based on constant stiffness space. In: Proceedings of 2019 IEEE International Conference on Robotics and Biomimetics (ROBIO). Dali: IEEE, 2019, 1041–1046
152. Gouttefarde M, Collard J F, Riehl N, Baradat C. Geometry selection of a redundantly actuated cable-suspended parallel robot. IEEE Transactions on Robotics, 2015, 31(2): 501–510
153. Jamwal P K, Hussain S, Xie S Q. Three-stage design analysis and multicriteria optimization of a parallel ankle rehabilitation robot using genetic algorithm. IEEE Transactions on Automation Science and Engineering, 2015, 12(4): 1433–1446
154. Zhang Z K, Shao Z F, Peng F Z, Li H S, Wang L P. Workspace analysis and optimal design of a translational cable-driven parallel robot with passive springs. Journal of Mechanisms and Robotics, 2020, 12(5): 051005
155. Zhang L X, Wang J S, Wang L P. Simplification of the rigid body dynamic model for a 6-UPS parallel kinematic machine under the accelerated motion and the decelerated motion. Journal of Mechanical Engineering, 2003, 39(11): 117–122
156. Staicu S. Dynamics analysis of the star parallel manipulator. Robotics and Autonomous Systems, 2009, 57(11): 1057–1064
157. Abdellatif H, Heimann B. Computational efficient inverse dynamics of 6-DOF fully parallel manipulators by using the Lagrangian formalism. Mechanism and Machine Theory, 2009, 44(1): 192–207
158. Yang C F, Huang Q T, He J F, Jiang H Z, Han J W. Model-based control for 6-DOF parallel manipulator. In: Proceedings of 2009 International Asia Conference on Informatics in Control, Automation and Robotics. Bangkok: IEEE, 2009, 81–84
159. Diao X M, Ma O. Vibration analysis of cable-driven parallel manipulators. Multibody System Dynamics, 2009, 21(4): 347–360
160. Khosravi M A, Taghirad H D. Dynamic analysis and control of cable driven robots with elastic cables. Transactions of the Canadian Society for Mechanical Engineering, 2011, 35(4): 543–557
161. Miermeister P, Pott A, Verl A. Dynamic modeling and hardware-in-the-loop simulation for the cable-driven parallel robot IPAnema. In: Proceedings of ISR 2010 (the 41st International Symposium on Robotics) and ROBOTIK 2010 (the 6th German Conference on Robotics). Munich: IEEE, 2010, 1–8
162. Piao J L, Jin X J, Jung J, Choi E, Park J O, Kim C S. Open-loop position control of a polymer cable–driven parallel robot via a viscoelastic cable model for high payload workspaces. Advances in Mechanical Engineering, 2017, 9(12): 1687814017737199
163. Piao J L, Jin X J, Choi E, Park J O, Kim C S, Jung J. A polymer cable creep modeling for a cable-driven parallel robot in a heavy payload application. In: Gosselin C, Cardou P, Bruckmann T,

Pott A, eds. Cable-Driven Parallel Robots. Cham: Springer, 2018, 62–72
164. Shao Z F, Tang X Q, Wang L P, Chen X. Dynamic modeling and wind vibration control of the feed support system in FAST. Nonlinear Dynamics, 2012, 67(2): 965–985
165. Miermeister P, Kraus W, Lan T, Pott A. An elastic cable model for cable-driven parallel robots including hysteresis effects. In: Pott A, Bruckmann T, eds. Cable-Driven Parallel Robots. Cham: Springer, 2015, 32: 17–28
166. Choi S H, Park K S. Integrated and nonlinear dynamic model of a polymer cable for low-speed cable-driven parallel robots. Microsystem Technologies, 2018, 24(11): 4677–4687
167. Ottaviano E, Castelli G. A study on the effects of cable mass and elasticity in cable-based parallel manipulators. In: Parenti Castelli V, Schiehlen W, eds. ROMANSY 18 Robot Design, Dynamics and Control. Vienna: Springer, 2010, 524: 149–156
168. Du J L, Bao H, Duan X C, Cui C Z. Jacobian analysis of a long-span cable-driven manipulator and its application to forward solution. Mechanism and Machine Theory, 2010, 45(9): 1227–1238
169. Du J L, Cui C Z, Bao H, Qiu Y Y. Dynamic analysis of cable-driven parallel manipulators using a variable length finite element. Journal of Computational and Nonlinear Dynamics, 2015, 10(1): 011013
170. Du J L, Agrawal S K. Dynamic modeling of cable-driven parallel manipulators with distributed mass flexible cables. Journal of Vibration and Acoustics, 2015, 137(2): 021020
171. Ferravante V, Riva E, Taghavi M, Braghin F, Bock T. Dynamic analysis of high precision construction cable-driven parallel robots. Mechanism and Machine Theory, 2019, 135: 54–64
172. Nguyen-Van S, Gwak K W, Nguyen D H, Lee S G, Kang B H. A novel modified analytical method and finite element method for vibration analysis of cable-driven parallel robots. Journal of Mechanical Science and Technology, 2020, 34(9): 3575–3586
173. Tempel P, Schmidt A, Haasdonk B, Pott A. Application of the rigid finite element method to the simulation of cable-driven parallel robots. In: Zeghloul S, Romdhane L, Laribi M, eds. Computational Kinematics. Cham: Springer, 2018, 50: 198–205
174. Liu Z H, Tang X Q, Shao Z F, Wang L P, Tang L W. Research on longitudinal vibration characteristic of the six-cable-driven parallel manipulator in FAST. Advances in Mechanical Engineering, 2013, 5: 547416
175. Du J L, Duan X C, Qiu Y Y. Dynamic analysis and vibration attenuation of cable-driven parallel manipulators for large workspace applications. Advances in Mechanical Engineering, 2013, 5: 361585
176. Do H D, Park K S. Analysis of effective vibration frequency of cable-driven parallel robot using mode tracking and quasi-static method. Microsystem Technologies, 2017, 23(7): 2577–2585
177. Yuan H, Courteille E, Gouttefarde M, Hervé P E. Vibration analysis of cable-driven parallel robots based on the dynamic stiffness matrix method. Journal of Sound and Vibration, 2017, 394: 527–544
178. Bao H, Duan B Y, Chen G D. Position control of 6-DOF cable-suspended parallel robotic with uncertain input. Journal of Mechanical Engineering, 2007, 43(7): 128–132 (in Chinese)
179. Lu Y J, Zhu W B, Ren G X. Feedback control of a cable-driven Gough–Stewart platform. IEEE Transactions on Robotics, 2006, 22(1): 198–202
180. Chellal R, Cuvillon L, Laroche E. A kinematic vision-based position control of a 6-DOF cable-driven parallel robot. In: Pott A, Bruckmann T, eds. Cable-Driven Parallel Robots. Cham: Springer, 2015, 32: 213–225
181. Zake Z, Chaumette F, Pedemonte N, Caro S. Vision-based control and stability analysis of a cable-driven parallel robot. IEEE Robotics and Automation Letters, 2019, 4(2): 1029–1036
182. Shang W W, Zhang B Y, Zhang B, Zhang F, Cong S. Synchronization control in the cable space for cable-driven parallel robots. IEEE Transactions on Industrial Electronics, 2019, 66(6): 4544–4554
183. Duan X C, Qiu Y Y, Duan B Y, Chen G D, Bao H, Mi J W. Adaptive interactive PID supervisory control of the macro-micro parallel manipulator. Journal of Mechanical Engineering, 2010, 46(1): 10–17 (in Chinese)
184. Gordievsky V. Design and control of a robotic cable-suspended camera system for operation in 3-D industrial environment. Dissertation for the Doctoral Degree. Cambridge: Massachusetts Institute of Technology, 2008
185. Baklouti S, Courteille E, Lemoine P, Caro S. Vibration reduction of cable-driven parallel robots through elasto-dynamic model-based control. Mechanism and Machine Theory, 2019, 139: 329–345
186. Abdelaziz S, Barbé L, Renaud P, de Mathelin M, Bayle B. Control of cable-driven manipulators in the presence of friction. Mechanism and Machine Theory, 2017, 107: 139–147
187. Najafi F, Bakhshizadeh M. Development a fuzzy PID controller for a parallel cable robot with flexible cables. In: Proceedings of 2016 the 4th International Conference on Robotics and Mechatronics (ICROM). Tehran: IEEE, 2016, 90–97
188. Khosravi M A, Taghirad H D. Robust PID control of fully-constrained cable driven parallel robots. Mechatronics, 2014, 24(2): 87–97
189. Zi B, Sun H H, Zhang D. Design, analysis and control of a winding hybrid-driven cable parallel manipulator. Robotics and Computer-Integrated Manufacturing, 2017, 48: 196–208
190. Babaghasabha R, Khosravi M A, Taghirad H D. Adaptive robust control of fully-constrained cable driven parallel robots. Mechatronics, 2015, 25: 27–36
191. Babaghasabha R, Khosravi M A, Taghirad H D. Adaptive robust control of fully constrained cable robots: singular perturbation approach. Nonlinear Dynamics, 2016, 85(1): 607–620
192. Tajdari F, Kabganian M, Rad N F, Khodabakhshi E. Robust control of a 3-DOF parallel cable robot using an adaptive neuro-fuzzy inference system. In: Proceedings of 2017 Artificial Intelligence and Robotics (IRANOPEN). Qazvin: IEEE, 2017, 97–101
193. Jabbari Asl H, Janabi-Sharifi F. Adaptive neural network control of cable-driven parallel robots with input saturation. Engineering Applications of Artificial Intelligence, 2017, 65: 252–260
194. Yu K, Lee L F, Tang C P, Krovi V N. Enhanced trajectory tracking control with active lower bounded stiffness control for cable robot. In: Proceedings of 2010 IEEE International

Conference on Robotics and Automation. Anchorage: IEEE, 2010, 669–674

195. Zarei M, Aflakian A, Kalhor A, Masouleh M T. Oscillation damping of nonlinear control systems based on the phase trajectory length concept: an experimental case study on a cable-driven parallel robot. Mechanism and Machine Theory, 2018, 126: 377–396
196. Jamshidifar H, Khosravani S, Fidan B, Khajepour A. Vibration decoupled modeling and robust control of redundant cable-driven parallel robots. IEEE/ASME Transactions on Mechatronics, 2018, 23(2): 690–701
197. Nishitani A, Inoue Y. Overview of the application of active/semiactive control to building structures in Japan. Earthquake Engineering & Structural Dynamics, 2001, 30(11): 1565–1574
198. Torres M A, Dubowsky S, Pisoni A C. Vibration control of deployment structures' long-reach space manipulators: the P-PED method. In: Proceedings of IEEE International Conference on Robotics and Automation. Minneapolis: IEEE, 1996, 2498–2504
199. Nenchev D N, Yoshida K, Vichitkulsawat P, Konno A, Uchiyama M. Experiments on reaction null-space based decoupled control of a flexible structure mounted manipulator system. In: Proceedings of International Conference on Robotics and Automation. Albuquerque: IEEE, 1997, 2528–2534
200. Yang T W, Xu W L, Tso S K. Dynamic modeling based on real-time deflection measurement and compensation control for flexible multi-link manipulators. Dynamics and Control, 2001, 11(1): 5–24
201. Staffetti E, Bruyninckx H, De Schutter J. On the invariance of manipulability indices. In: Lenarčič J, Thomas F, eds. Advances in Robot Kinematics. Dordrecht: Springer, 2002, 57–66
202. Tang X Q, Chai X M, Tang L W, Shao Z F. Accuracy synthesis of a multi-level hybrid positioning mechanism for the feed support system in FAST. Robotics and Computer-Integrated Manufacturing, 2014, 30(5): 565–575
203. Rushton M, Khajepour A. Transverse vibration control in planar cable-driven robotic manipulators. In: Gosselin C, Cardou P, Bruckmann T, Pott A, eds. Cable-Driven Parallel Robots. Cham: Springer, 2018, 53: 243–253
204. de Rijk R, Rushton M, Khajepour A. Out-of-plane vibration control of a planar cable-driven parallel robot. IEEE/ASME Transactions on Mechatronics, 2018, 23(4): 1684–1692
205. Rushton M, Jamshidifar H, Khajepour A. Multiaxis reaction system (MARS) for vibration control of planar cable-driven parallel robots. IEEE Transactions on Robotics, 2019, 35(4): 1039–1046
206. Korayem M H, Yousefzadeh M, Manteghi S. Tracking control and vibration reduction of flexible cable-suspended parallel robots using a robust input shaper. Scientia Iranica, 2018, 25(1): 230–252
207. Montgomery F, Vaughan J. Suppression of cable suspended parallel manipulator vibration utilizing input shaping. In: Proceedings of 2017 IEEE Conference on Control Technology and Applications (CCTA). Maui: IEEE, 2017, 1480–1485
208. Liebherr. High-tensile fibre rope for tower cranes. Available from Liebherr website, 2021
209. Lau D, Eden J, Tan Y, Oetomo D. CASPR: a comprehensive cable-robot analysis and simulation platform for the research of cable-driven parallel robots. In: Proceedings of 2016 IEEE/RSJ International Conference on Intelligent Robots and Systems (IROS). Daejeon: IEEE, 2016, 3004–3011
210. Pott A. WireX: an open source initiative scientific software for analysis and design of cable-driven parallel robots. In: Proceedings of Fourth International Conference on Cable-driven Parallel Robots. Krakow, 2019